

**HIGH-RESOLUTION TEMPORAL SOLAR IRRADIANCE
MEASUREMENT**

CHEAH KAI YUEN


**A project report submitted in partial fulfilment of the
requirements for the award of Bachelor of Engineering
(Honours.) Electrical and Electronics Engineering**

**Lee Kong Chian Faculty of Engineering and Science
Universiti Tunku Abdul Rahman**

May 2020

DECLARATION

I hereby declare that this project report is based on my original work except for citations and quotations which have been duly acknowledged. I also declare that it has not been previously and concurrently submitted for any other degree or award at UTAR or other institutions.

Signature :  _____

Name : CHEAH KAI YUEN _____

ID No. : 16 UEB 03770 _____

Date : 14/5/2020 _____

APPROVAL FOR SUBMISSION

I certify that this project report entitled “**HIGH-RESOLUTION TEMPORAL SOLAR IRRADIANCE MEASUREMENT**” was prepared by **CHEAH KAI YUEN** has met the required standard for submission in partial fulfilment of the requirements for the award of Bachelor of Engineering (Honours.) Electrical and Electronics at Universiti Tunku Abdul Rahman.

Approved by,

Signature : 

Supervisor : DR. LIM BOON HAN

Date : 15 May 2020

Signature : -

Co-Supervisor : -

Date : -

The copyright of this report belongs to the author under the terms of the copyright Act 1987 as qualified by Intellectual Property Policy of Universiti Tunku Abdul Rahman. Due acknowledgement shall always be made of the use of any material contained in, or derived from, this report.

© 2020, Cheah Kai Yuen. All right reserved.

ACKNOWLEDGEMENTS

I would like to thank everyone who had contributed to the successful completion of this project. I would like to express my gratitude to my research supervisor, Dr. Lim Boon Han for his invaluable advice, guidance and his enormous patience throughout the development of the research.

In addition, I would also like to express my gratitude to my loving parents and friends who had helped and encouraged me during the whole final year project.

ABSTRACT

Nowadays, electricity had become an important part in our daily life. Electricity that we used currently is mostly generated by combustion of fossil fuel. These fossil fuels are non-renewable and will pollute the environment during combustion to generate electricity. Thus, scientists are focusing on harvesting renewable energy such as solar, wind and tides energy in order to replace the non-renewable energy and at the same time reduce air pollution. In Malaysia, solar PV panel is most suitable to be installed to harvest solar energy since it is located near the equator and has tropical weather. A high-resolution temporal solar irradiance measurement is needed to study the intermittency of solar power as it has a higher sampling rate. Intermittency is defined as the unavailability of renewable energy power source in a certain period of time. Low resolution measurement system may overlook the intermittency. In this paper, a 10 seconds resolution solar irradiance measurement system is built and the collected data is automatically uploaded to the cloud for storage. The results obtained from the sensor in 10 seconds basis were compared with the minute basis results from the pyranometer. Other than that, another two circuits with the same configuration are also built and calibration had been made for each system. These three systems are used to study about intermittency in the future. Besides that, the data which is collected in 15 days from 19 March 2020 to 2 April 2020 is analysed. Standard deviation and maximum difference between points for 10seconds, 20 seconds, 30seconds, 1 minute, 2 minutes and 5 minutes measurement time resolution are calculated and plotted.

TABLE OF CONTENTS

DECLARATION		i
APPROVAL FOR SUBMISSION		ii
ACKNOWLEDGEMENTS		iv
ABSTRACT		v
TABLE OF CONTENTS		vi
LIST OF TABLES		viii
LIST OF FIGURES		ix
LIST OF SYMBOLS / ABBREVIATIONS		xiii
LIST OF APPENDICES		xiv
 CHAPTER		
1	INTRODUCTION	1
	1.1 Background	1
	1.2 Importance of the Study	3
	1.3 Problem Statement	4
	1.4 Aim and Objectives	4
	1.5 Scope and Limitation of the Study	5
2	LITERATURE REVIEW	6
	2.1 Introduction	6
	2.2 Literature Review	6
	2.2.2 Measurement models for predicting the irradiance variability.	7
	2.2.3 Collection of real-time environment data using Raspberry Pi.	9
	2.2.4 High-resolution solar radiation measurement in Singapore	10
	2.2.5 The differences of high-resolution solar irradiance data collection between ground and satellite-derived.	13

	2.2.6	Generation of Solar Irradiance Data at 10 minutes basis using a new technique.	14
	2.2.7	How solar irradiance intermittency influences the Photovoltaic system.	16
	2.2.8	The effect of compensation of photovoltaic system with the grid to help to improve the voltage drop problem.	19
3		METHODOLOGY AND WORK PLAN	22
	3.1	Overview	22
	3.3	Raspberry Pi 3B+	24
	3.4	Setting up Raspberry Pi	25
	3.5	NES Silicon Solar Radiation Sensor Type SOZ-03	27
	3.6	DS18B20	28
	3.7	MCP3002	29
	3.8	Coding	30
	3.9	Method of Measurement	31
		3.9.1 Method of collecting data	31
		3.9.2 Method of Analysing data	33
	3.10	Work plan and Gantt chart	34
4		RESULTS AND DISCUSSION	36
	4.1	Comparison between Raspberry Pi data and Pyranometer's data	36
		4.1.1 Graph Comparison with pyranometer	36
	4.2	Data logging with overGrive	38
	4.3	Duplicating of three sets of circuits.	39
	4.4	Analysing the collected data from Set to comparing to different time resolution.	42
5		CONCLUSION AND RECOMMENDATION	47
	5.1	Conclusion	49
	5.2	Future improvement	50

LIST OF TABLES

Table 1: Comparison between Arduino and Raspberry Pi(What are the differences between Raspberry Pi and Arduino?, 2017)	25
Table 2: Specification of SOZ-03 Silicon Solar Radiation Sensor	27
Table 3: Specification of DS18B20	28
Table 4: Specification of MCP 3002	29

LIST OF FIGURES

- Figure 1: zenith angle. 2
- Figure 2: SUNY-modelled and monthly-averaged daily DNI for 37 stations. (Gueymard and Wilcox, 2009) 7
- Figure 3: Block diagram of Raspberry Pi-based DAS (Sharma et al., 2017) 10
- Figure 4: Variation of diffused and global horizontal radiation observed in 10 minutes on 1 September 2010. (Jayaraman and Maskell, 2012) 11
- Figure 5: The direct beam measurements of two different stations on 14 September 2010 between 07:00 and 18:59 to investigate spatial variation (Jayaraman and Maskell, 2012) 12
- Figure 6: Comparison of the direct beam measurements from the two different stations on 14 September 2010 within 14:00 and 14:59 (Jayaraman and Maskell, 2012) 12
- Figure 7: Comparison between synthetic and real data in January. (Hontoria et al., 2019) 15
- Figure 8: Comparison between synthetic and real data in April. (Hontoria et al., 2019) 15
- Figure 9: Comparison between synthetic and real data in July. (Hontoria et al., 2019) 16
- Figure 10: Simulated results of solar irradiance and PV current by McCormick. (McCormick and Suehrcke, 2018) 17
- Figure 11: Graph of current from all devices vs the local time. (McCormick and Suehrcke, 2018) 18
- Figure 12: Graph of solar irradiance vs local time and graph of battery current vs local time in hour and minute basis. (McCormick and Suehrcke, 2018) 19

Figure 13: Graph of battery current vs local time in minute and hourly basis. (McCormick and Suehrcke, 2018)	19
Figure 14: Graph of voltage drop vs the length of transmission line between transformer and load before installation of PV systems. (Mouheb, Hamidat, and Loukarfi, 2012)	20
Figure 15: Graph of voltage drop vs the length of transmission line between transformer and load after installation of several PV systems. (Mouheb, Hamidat, and Loukarfi, 2012)	21
Figure 16: The effect on the current produced before and after the installation of PV systems. (Mouheb, Hamidat and Loukarfi, 2012)	21
Figure 17: Block diagram of the whole circuit construction.	22
Figure 18: Circuit diagram	23
Figure 19: Raspberry Pi 3B+	24
Figure 20: Command to update the Raspberry Pi	26
Figure 21: SOZ-03 Silicon Solar Radiation Sensor Type	27
Figure 22: DS18B20	28
Figure 23: MCP 3002	29
Figure 24: Circuit which is built for testing the functionality of MCP3002 and recording the surrounding temperature	32
Figure 25: Comma-separated value file to record the irradiance and temperature data on 1 st Dec 2019.	32
Figure 26: Comparison of data on 1.12.2019. Ky is the data collected by the Raspberry Pi circuit while Pyr is the data collected by the pyranometer.	36
Figure 27: Comparison of data on 15.12.2019. Ky is the data collected by the Raspberry Pi circuit while Pyr is the data collected by the pyranometer.	37

- Figure 28: Comparison of data on 31.12.2019. Ky is the data collected by the Raspberry Pi circuit while Pyr is the data collected by the pyranometer. 37
- Figure 29: Solar irradiance data stored in Google Drive. 39
- Figure 30: Graph comparison between the first set and the second set circuit. The blue line represents set 1 while the orange line represents set 2. 40
- Figure 31: Percentage difference between the first and the second circuit from 8:00 to 18:00 on 9.3.2020. 40
- Figure 32: Graph of comparison between Set 2 and Set 3 on 19.3.2020. The blue line represents Set 2 while the orange line represents Set 3. 41
- Figure 33: Percentage difference of second and third circuit from 8:00 to 18:00 on 19.3.2020 42
- Figure 34: Graph of comparison between 10-seconds data with 1-minute data. 43
- Figure 35: Graph of comparison between 10-seconds data with 5-minutes data. 44
- Figure 36: Graph of comparison between 10-seconds data with 30-minutes data. 44
- Figure 37: Graph of standard deviation against time resolution for 15 days. The time resolutions are 10-seconds, 20-seconds, 30-seconds, 1 minute, 2 minutes, and 5 minutes. 46
- Figure 38: Graph of the standard deviation of changes in solar irradiance. The time resolutions are 10-seconds, 20-seconds, 30-seconds, 50-seconds, 1 minute, 2 minutes, and 5 minutes. 46
- Figure 39: Graph of maximum solar irradiance difference between points against date. It compares between 10 seconds, 20 seconds, 30 seconds, 50 seconds, 1 minute, 2 minutes, and 5 minutes. 47
- Figure 40: Graph of frequency of solar irradiance changes that is higher than 100 W/m^2 against different

time resolutions. It compares between 10 seconds, 20 seconds, 30 seconds, 50 seconds, 1 minute, 2 minutes, and 5 minutes. 48

LIST OF SYMBOLS / ABBREVIATIONS

PV	Photovoltaic
DNI	Direct Normal Irradiance
DHI	Diffuse Horizontal Irradiance
GHI	Global Horizontal Irradiance
LCOE	Lowest Levelized Cost of Energy
ROI	Return of Investment
WVM	Wavelet Variability Method
DAS	Data Acquisition System
HRIA	High-Resolution Irradiance Algorithm
SIND	Solar Integration National Database
ADC	Analogue-to-Digital
SPI	Serial Peripheral Interface
VNC	Virtual Network Computing
SSH	Secure Shell

LIST OF APPENDICES

APPENDIX A:10 seconds solar irradiance measurement coding	50
---	----

CHAPTER 1

INTRODUCTION

1.1 Background

Renewable energy is one of the main topics that are discussed in the engineering field recently to reduce pollution levels such as air pollution. Fossil fuels which are burned to produce energy and electricity release carbon which is harmful to human and causes air pollution. Many industries and governments around the world are working hard to find solutions to cut down greenhouse gases emission by implementing renewable energy system. Renewable energy such as solar energy can be replenished. Technology regarding solar energy has emerged within these few decades. It is preferred as it is more convenient to be installed and most suitable for Malaysia's environment. Malaysia is located near to the equator and receives average solar insolation of 400 to 600 MJ/m² monthly. The amount of solar irradiance collected is higher from October to March and is lower from April to September every year. (Mekhilef et al., 2012). The advantages of solar PV system include it has no moving parts, direct conversion from light energy to electrical energy, last for an extended, low maintenance costs and suitable for space applications such as satellites. (Singh, 2013)

In order to determine whether a site is suitable for installing a PV system, the measurement of solar irradiance is one of the most critical issues. Solar irradiance can be categorized into direct normal irradiance, diffuse horizontal irradiance, and global horizontal irradiance. Direct normal irradiance (DNI) is the amount of direct irradiance which is collected per unit area by a plane that is placed perpendicular to the sun. (Blanc et al., 2014). Diffuse horizontal irradiance (DHI) is explained as the solar irradiance which had been diffused by dust or other particles in the surrounding and collected at the certain unit area. During the cloudy day, a significant portion of irradiance collected is DHI instead of DNI. (Hejase and Assi, 2016). Next, the global horizontal irradiance (GHI) is defined as the shortwave irradiance transmission which is the sum of DNI and DHI. The formula for GHI is shown in Equation (1). z is the zenith angle. It is calculated by $90^\circ -$ elevation angle of the solar ray to the surface of the detector's surface as shown in Figure 1.

$$GHI = DHI + DNI \cos(z) \quad (1)$$

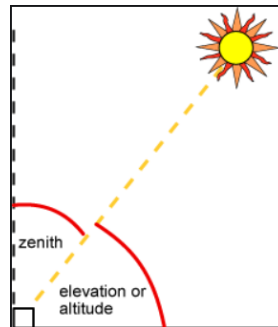


Figure 1: zenith angle.

The solar irradiance value will vary due to the movement of clouds, the quality of air, and the presence of tall plants. The clearness index is the ratio of transmitted solar irradiance on the Earth to the extraterrestrial radiation. On the other hand, the clear sky index is the ratio of the intensity of ground irradiance to the predicted irradiance during unclouded days. Besides that, the condition of the surrounding air will affect the solar irradiance collection as the sunlight transmitted to the Earth may diffuse after hitting on the air pollutants such as dust, particulate matter and nitrates, and sulphates. The shadows of trees will also block the solar intensity from reaching the ground if a PV panel is placed under the shadow. (Rathod, Mittal and Kumar, 2017) The areas that receive low solar irradiance will have a larger total current harmonic distortion compared to the total voltage harmonic distortion. (Patsalides et al., 2007)

Besides that, researches done on the intermittency of solar irradiance is also crucial to forecast the characteristic of irradiance at a particular solar farm. Intermittency of solar irradiance is defined as the fluctuation of solar irradiance at a specific area within a range of time (Vindel and Polo, 2014). The intermittency that happens may be due to shading. The effect of intermittency of solar irradiance is that it may cause a sudden voltage drop from the output of a PV plant. This voltage drop may cause inconvenience to the user. Hans Georg Beyer states that there is a need to improve the amount of data collected within a specific period in his article. (Beyer et al., 1991). Matthew Lave and Andrew Weekly stated that the collection of high-frequency solar variability is still limited. The results generated by low resolution temporal solar irradiance

measurement such as an hour or a month has an error of 27%. (Lave and Weekley, 2017). In order to obtain a complete dataset, a higher resolution solar irradiance measurement system had to be developed. This system should be able to collect a more substantial amount of solar irradiance data within a fixed period, store the data collected to cloud storage, and convenient for the users to access the collected data even though they are away from the solar site.

1.2 Importance of the Study

Since solar energy has become one of the most important renewable energy in this world, the accuracy of solar irradiance's measurement also becomes very important. If the irradiance data collected is not accurate enough, the estimated output power produced by the PV farm will be affected severely. Lastly, it may also affect the calculation of the payback time. Measurement of solar irradiance is vital to determine the Lowest Levelized cost of energy (LCOE) and the highest return of investment (ROI). The most common method to measure solar irradiance is using solar irradiance meter.

A data logger is used to store the solar irradiance data collected. A data logger that can upload the data to the cloud for storage is quite expensive. Thus, a new data logger with a lower cost to store data to the cloud and has a higher resolution has to be created.

Besides that, the study of ambient temperature is important because the performance of the panel will drop with the increase in temperature, especially in tropical countries. The power loss can reach 10% to 18%. In a study done by Lai Keen Yip, he estimated the PV modules temperature by implementing two module temperature models which are the time-specific Ross coefficient and overall Ross coefficient. The Ross coefficient is proportional to the increment of solar irradiance. In Lai's study, he found out that the temperature of the module should be the same as the temperature of the surroundings when there is no sunlight exists. He proved that the y-intercept points of Ross coefficient should be included in Ross equation so that the temperature of the module within the high module temperature period can be detected. He also proved that with time-specific values of Ross coefficient have more accurate generated data compared to using the overall Ross coefficient. (Lai, n.d.)

Throughout this study, more data can be collected as the higher resolution temporal solar irradiance measurement of 10 seconds is implemented and the data can be stored to the cloud. With more data collected, the intermittency of solar irradiance can also be studied.

1.3 Problem Statement

High-frequency solar irradiance measurement of 10 seconds or shorter is important to study the effect of the solar PV system to a distribution grid. The error in getting accurate data will be as high as 70% if low-resolution solar variability of 15 minutes is applied. (Lave, Reno and Broderick, 2015). Besides that, while sizing an inverter, the temporal resolution of solar irradiance cannot be too high or too low. It should be within the range of one hour and ten seconds. A research was done by Song Chen and his team with the resolution of one minute. (Chen and Brady, 2010). Since the current temporal resolution applied in SOLARGIS database is 15 minutes, it has to be improved to a smaller sampling interval to obtain more accurate data. (Solargis global solar radiation data / Time Series and TMY / Tech Specs | Solargis, 2019).

Thus, a higher-resolution measurement of solar irradiance is needed to understand the intermittency characteristic of solar intensity strength and to get a more accurate solar irradiance data. Intermittency of solar energy will cause voltage drop from the solar panel and thus affects the electricity supply. With a higher resolution measurement, the data collected will increase and huge storage shall be used to store these data.

1.4 Aim and Objectives

This project is the study about the method to enhance the reliability and stability of a PV system by analyzing the data collected every 10 seconds. The collected data is compared with data with lower resolutions.

- To set up a solar irradiance sensor system using Raspberry Pi 3B+ as the microprocessor that can collect data every 10 seconds.
- To store the data collected to cloud storage.
- To analyze the data collected for increasing the reliability of a PV system.

1.5 Scope and Limitation of the Study

This project will cover the construction of the whole solar irradiance sensor system and the installation of the system at the solar sites. The type of solar irradiance sensor used in this project is the monocrystalline silicon solar irradiance sensor. The data obtained is compared with the data released by the online solar irradiance database. In Chapter 2, literature reviews will discuss different models which are used to measure and determine the solar irradiance. Besides that, Raspberry-Pi based weather station will also be discussed.

There are some limitations to this project. First, in this project, only monocrystalline silicon type solar irradiance sensor is used. Since the pyranometer uses a different type of irradiance sensor material and 1-minute temporal measurement resolution, the results will have a slight difference when compared. However, the characteristic of the graph of solar irradiance against time should be the same. Besides that, the time for collecting data is quite limited which is six months.

CHAPTER 2

LITERATURE REVIEW

2.1 Introduction

In order to determine the reliability of a solar system, the measurement of solar irradiance is a must factor. Lots of studies had been revised regarding solar irradiance and different methods are developed to collect the irradiance data. Some of the methods are included in the literature review. Besides that, In Malaysia, a fixed position solar panel may not collect the maximum amount of irradiance as the sun's position varies in different months in a year

2.2 Literature Review

2.2.1 Solar temporal and spatial characteristics.

Solar energy is the main energy that maintains the life of all the living organisms on Earth. It is a limitless supply. That is why people start to utilize it to generate energy to supply power to equipment. However, in order to generate sufficient energy to replace non-renewable energy, it requires a very constant and continuous supply of solar irradiance. Several factors will affect the amount of solar irradiance which reaches the ground. The intermittency of solar energy is caused by two main reasons, which are the accuracy in detecting the position and path of the sun, the accurate distance between the earth and the sun, and the movements of clouds. Solar irradiance always changes with time and space. In order to confirm the solar irradiance data collected at a specific site is accurate, data need to be collected for more than 30 years and analyzed. Besides that, while collecting solar irradiance data, some hours of data will be lost or had to be reanalyzed due to the reliability of the data collecting system error. According to statistics, at least 25% of data is lost per month. It is shown in Figure 2. (Gueymard and Wilcox, 2009)

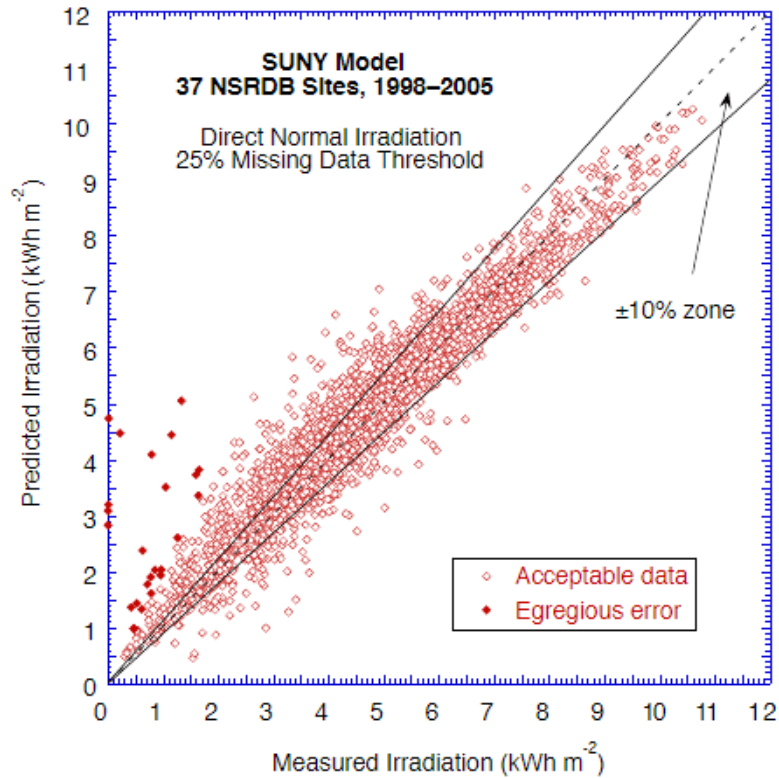


Figure 2: SUNY-modelled and monthly-averaged daily DNI for 37 stations. (Gueymard and Wilcox, 2009)

In terms of spatial characteristics, if solar energy can be collected or harvested in a broader region, the intermittency will be reduced. If the whole world implements solar farms to generate energy, then the intermittency will be cancelled entirely. Temporal characteristic means that the time interval for collecting irradiance data. The solar irradiance may have different values every single second. The variability of irradiance depends on the clearness index, Kt , and clear sky index, Kt^* . The clearness index refers to the ratio of GHI to the extraterrestrial radiation while the clear sky index means the ratio of GHI to the cloudless day solar radiation. (Perez et al., 2016)

2.2.2 Measurement models for predicting the irradiance variability.

Three approaches had been proposed to foresee solar radiation variability. First, Lave et al. developed the wavelet variability method (WVM) to disintegrate the irradiance impulse data into different time frames to determine the power output. This method uses the inputs from a solar irradiance sensor, the understanding of a solar plant and the output power of PV per m^2 , daily cloud speed, and spatio-

temporal correlation function to predict the ratio of fluctuation of solar irradiance at a specific plant site.

Next, the second model was developed by Hoff and Perez and it computes the variances of the sum of possible solar site pair in a PV fleet.

$$\sigma_{\Delta t}^{fleet} = \sqrt{Var \sum_{n=1}^N \Delta P_{\Delta t}^n} = \sqrt{\sum_{i=1}^N \sum_{j=1}^N COV(\Delta P_{\Delta t}^i, \Delta P_{\Delta t}^j)} \quad (2.1)$$

Since the multiplication of the variance of each location with the correlation coefficient between two locations is equal to the covariance between two solar plants, Equation (2.1) can be simplified into Equation (2.2). The main concern for Equation (2.2) is the interrelation between every plant and the output power of a single plant.

$$\sigma_{\Delta t}^{fleet} = \sqrt{\sum_{i=1}^N \sum_{j=1}^N \sigma_{\Delta t}^i \sigma_{\Delta t}^j \rho_{\Delta t}^{i,j}} \quad (2.2)$$

Representative block method was developed by Kato et al. This method is used to determine the variation in a high-penetration photovoltaic system over a defined broad area. These PV plants are then separated into small groups and with N numbers of blocks. These blocks have specific variability and output. The interrelation between the blocks is set so that they can be ignored. A new equation was defined and shown in Equation (2.3).

$$Fleet \text{ relative variability} = \frac{\sqrt{N} \sigma(\Delta p_{\Delta t})}{N P_{installed}} \quad (2.3)$$

The satellite generated solar irradiance data is more accurate compared to linear interpolation method data as it has a more continuous collection of data with a shorter temporal resolution and smaller spatial resolution. (Perez et al., 2016)

2.2.3 Collection of real-time environment data using Raspberry Pi.

A microcontroller or microprocessor is needed for data acquisition. Data acquisition is defined as converting analog data into digital form. After converting the data, a microprocessor is used to read, analyze, and store them. The environment data collected is useful for engineers or scientists during research. Data acquisition system (DAS) can be divided into 3 sections, which are the input or output subsystem, main computer, and software. A prototype had been created by Davinder Pal Sharma to collect environment data using Raspberry Pi B+ as the host microprocessor. Their system can obtain the rain level, wind speed and direction, solar irradiance, temperature, and humidity data. DHT-11 is to measure the temperature and humidity of the environment. However, the accuracy of the output produced by this sensor is low. Thus, it needs to be calibrated frequently. In order to obtain solar irradiance data, CM-11 Kipp & Zonen Pyranometer is used. The output of this sensor needs to be amplified before transferring into an ADC circuit and Raspberry Pi.

The most common programming language used in Raspberry is Python as it is more readable compared to others and object-oriented. The block diagram of the prototype from Davinder is shown in Figure 3. All the data collected is sent to the Raspberry Pi. After processing the data, Raspberry Pi will send the data to Web Server for easy real-time access. PHP programming language is used to create web content to act as a server to access the database. PHPMyAdmin tool will allow MySQL to connect to the web browser. MySQL will edit, add, and access the database created. Raspberry Pi based weather station is cheaper compared to most of the weather stations and it can collect real-time data. The disadvantage of the system is the error percentage is high. This is due to the accuracy of the sensors used and system error margins. (Sharma et al., 2017)

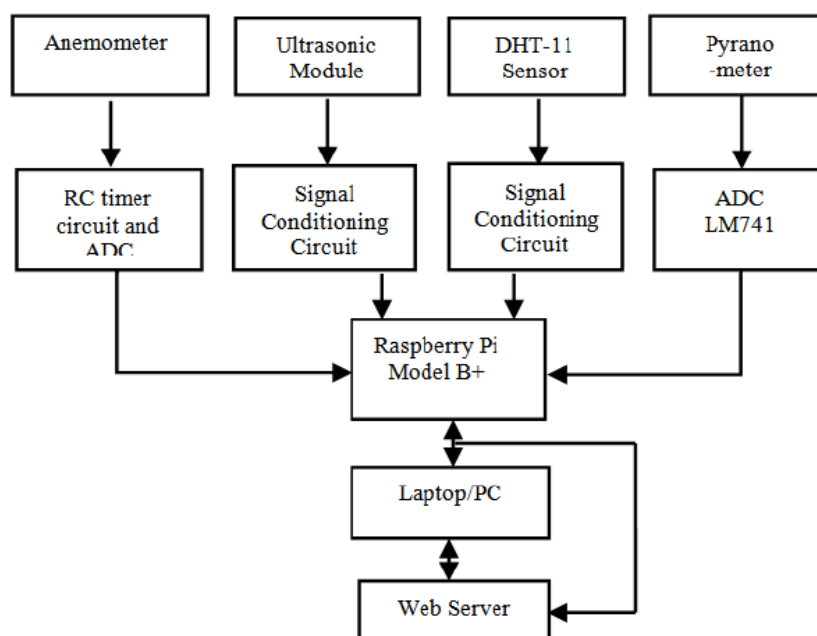


Figure 3: Block diagram of Raspberry Pi-based DAS (Sharma et al., 2017)

2.2.4 High-resolution solar radiation measurement in Singapore

The movement of clouds will cause spatial and temporal variation in solar insolation patterns. A short-term variation of solar irradiance will affect the efficiency of photovoltaic and concentrator photovoltaic systems. Thus, a high resolution spatial and temporal solar radiation measurement system should be designed. Since the cost for instruments and materials to build a solar measurement system is high, a low cost and uncomplicated method are tested by Ramkumar Jayaraman to measure the radiant energy radiated from the Sun. According to his studies, there is a common shortcoming with the works which are done by researches earlier. The drawback is that their projects have sampling intervals between an hour and one month. These intervals are too long to get an accurate result. This is proven in articles from Gansler RA and Gayathri Vijayakumar. These articles show that the imprecise output was generated using an hourly-correlation defined diffuse fractions. A diffuse fraction is defined as the ratio of measured horizontal radiation to extraterrestrial radiation on a normal surface for a constant extent of time.

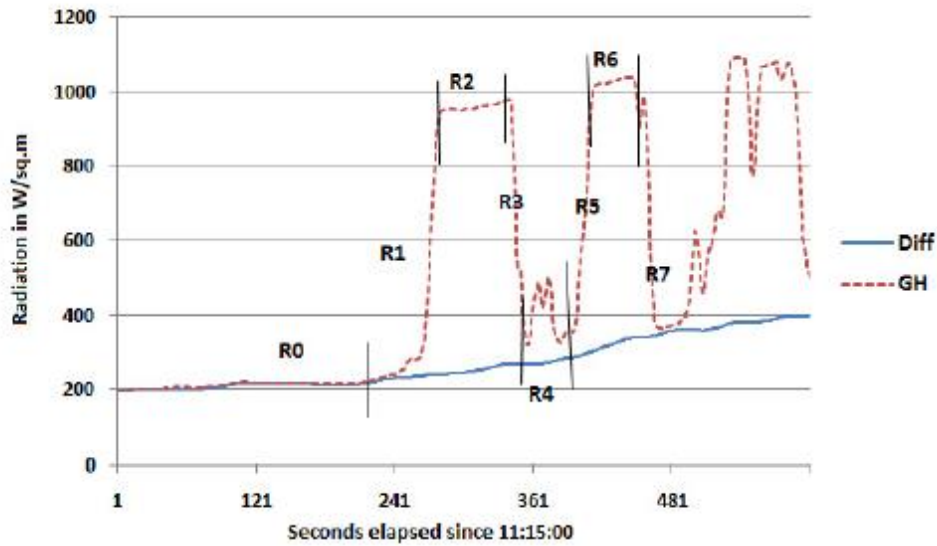


Figure 4: Variation of diffused and global horizontal radiation observed in 10 minutes on 1 September 2010. (Jayaraman and Maskell, 2012)

Based on Figure 4, the fluctuation in diffuse solar radiation is small compared to global horizontal radiation, GH. GH graph in Figure 4 is separated into 8 sections, from R0 to R7. R2, R4, and R6 is the steady-state condition. During steady-state, the controller was unable to detect the variation of solar insolation. Therefore, the time range for the transient and characteristics of solar insolation during steady-state will affect the solar PV and concentrator PV system. The existing of the transient is due to many factors such as shape, type, height, and speed of movement of the cloud.

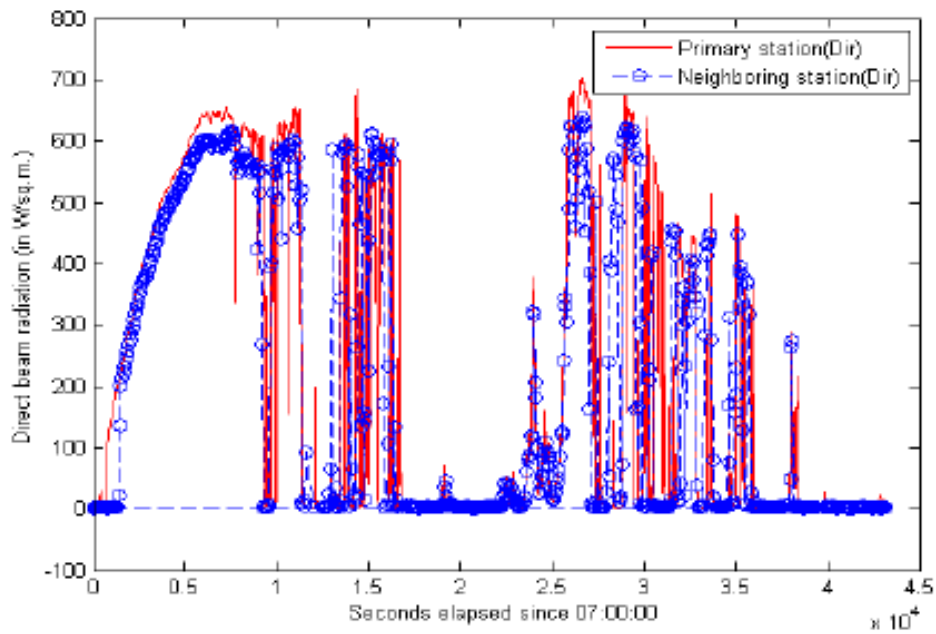


Figure 5: The direct beam measurements of two different stations on 14 September 2010 between 07:00 and 18:59 to investigate spatial variation (Jayaraman and Maskell, 2012)

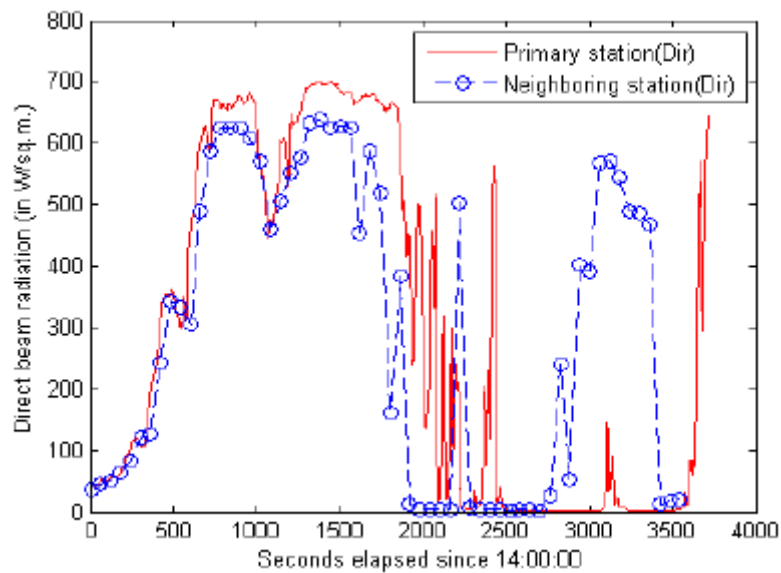


Figure 6: Comparison of the direct beam measurements from the two different stations on 14 September 2010 within 14:00 and 14:59 (Jayaraman and Maskell, 2012)

In order to study the spatial characteristic of direct, diffuse and global horizontal radiation, measurements from two weather stations which is near to each other are compared. According to Figures 5 and 6, transient and spatial variation will cause significant changes in direct radiation. In conclusion, the direct and global horizontal radiation will have significant variation due to the movement of clouds. Other than that, the temporal and spatial variation has a small effect on diffuse radiation across a range of 500m. Thermopile used throughout the project can be replaced with low-cost silicon sensors in order to obtain a more accurate solar insolation data with temporal and spatial changes and cut down the budget. (Jayaraman and Maskell, 2012)

2.2.5 The differences of high-resolution solar irradiance data collection between ground and satellite-derived.

High-resolution irradiance algorithm (HRIA) is a method discovered by National Renewable Energy Laboratory to generate a 4-second resolution global irradiance data using the satellite-derived data. However, it is still under the research's stage. High-resolution solar irradiance measurement is dominant for studies regarding the effect of the PV systems on a grid. Researches about high-resolution ground-measured irradiance are still insufficient. Based on the research done by Matthew Lave and his team about the comparison between the high temporal resolution of load and PV variability, the high-resolution irradiance measurement has to be implemented instead of low-resolution measurement as the percentage error discovered when low-resolution data is applied in their research is up to 27%. (Lave et al., 2017)

The Solar Integration National Database (SIND) method is applied so that the satellite can collect the solar irradiance data at a faster rate from 30 minutes to 1 minute. The data collection rate can be scaled down further to 4 seconds by applying the Fourier transform. There will be a slight difference between the solar irradiance measured using ground measurement with the satellite-derived irradiance data. This is because the method that is used to measure the variability of solar irradiance is different for both satellite and ground measurement. The exact time for the two systems to detect the existence of the clouds is also different.

A metric named daily variability score is used to measure the solar variability. Matthew Lave and Andrew Weekly had made a comparison between the data obtained by ground measurement of Sandia's database and HRIA with a resolution of 30-seconds. They concluded that during the clear day, HRIA's data and ground-measured data are almost similar. However, during cloudy days, HRIA variability score and ground measurement variability score are different. (Lave and Weekley, 2017)

2.2.6 Generation of Solar Irradiance Data at 10 minutes basis using a new technique.

Several methods had been proposed to analyze the solar irradiance data in a shorter time scale. However, these techniques are quite complicated and hard to establish. Some new ideas such as the "smart city" require a higher temporal resolution solar irradiance data if they plan to implement photovoltaic technology in the system. Currently, the common resolution of solar irradiance measurement is in daily and hourly basis.

Before creating a mathematical model to generate synthetic solar irradiance data for comparison, two main characteristics must be included, which are the independent characteristics of solar irradiance time and time-dependent characteristics of solar irradiance. Klein designed a solution that uses the clarity index to remove the changes in irradiance data due to the four seasons. However, this method only focuses on the clarity index but not the actual global irradiance. Besides that, the model developed by Graham and Hollands based in Gaussian inversion techniques and Markov Transition Matrices model by Aguiar and Collares-Pereira is a famous model. Other than the methods stated, there is another method called ARIMA (AutoRegressive Integrated Moving Average), which is the most suitable technique for generating hourly and every minute's weather data.

Leocadio Hontoria and his team analyzed the solar irradiance data from a database in Jaén, Spain. After determining the two main characteristics as mentioned, the Typical Meteorological Year (TMY) was calculated. Typical Meteorological Year collects global horizontal irradiance (GHI) and surrounding temperature on an hourly basis throughout a year. They analyzed and compared the synthetic and real solar irradiance data for January, April, and

July at a solar site in Jaén, Spain. The results of their experiments are shown in Figures 7, 8 and 9. (Hontoria et al., 2019)

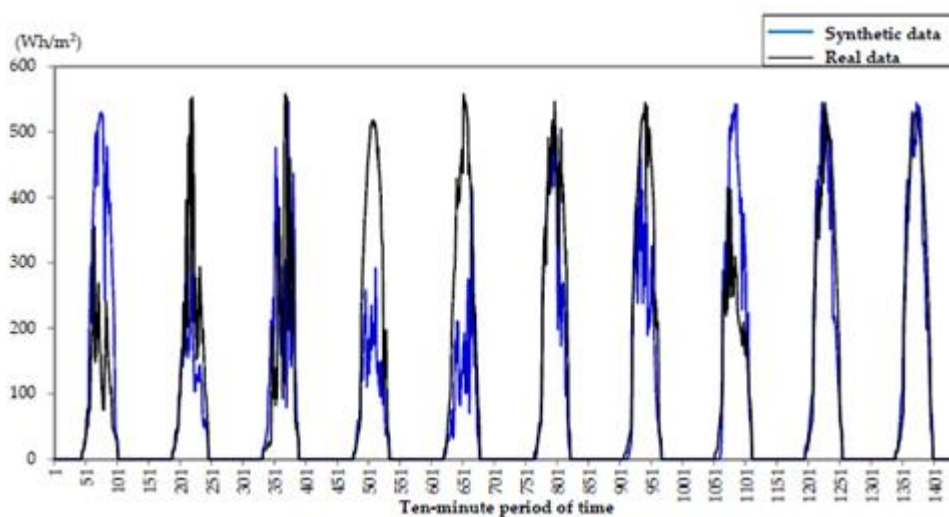


Figure 7: Comparison between synthetic and real data in January. (Hontoria et al., 2019)

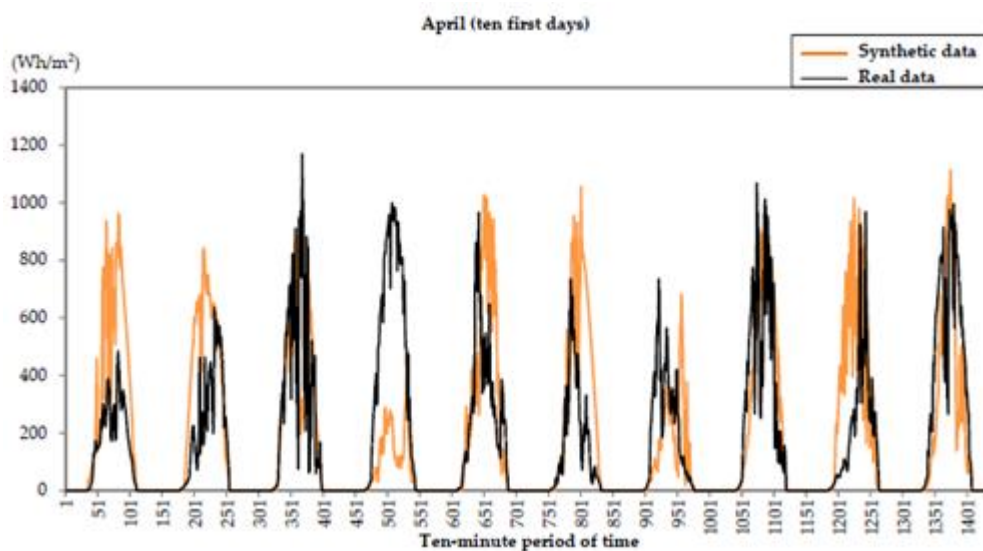


Figure 8: Comparison between synthetic and real data in April. (Hontoria et al., 2019)

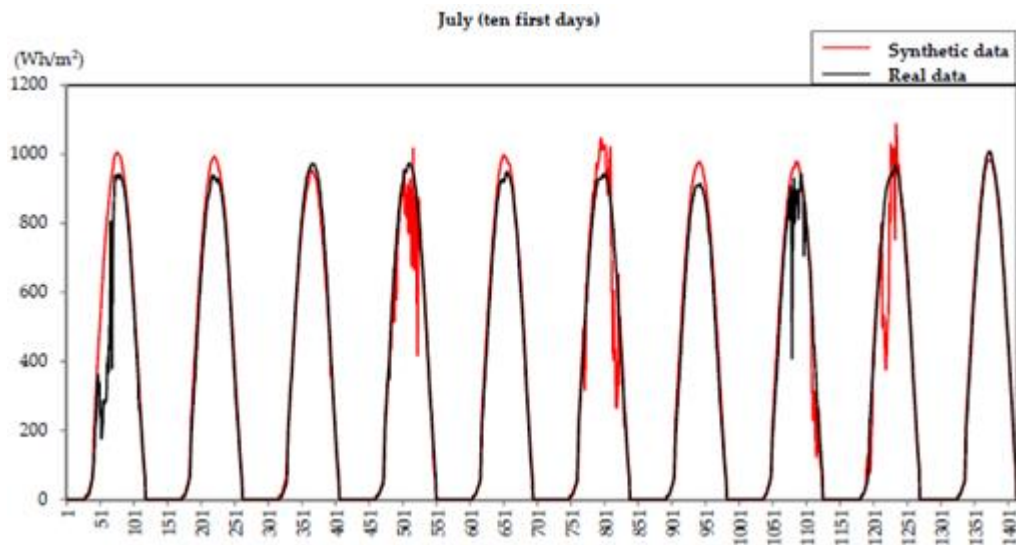


Figure 9: Comparison between synthetic and real data in July. (Hontoria et al., 2019)

2.2.7 How solar irradiance intermittency influences the Photovoltaic system.

The difference between the performance of a photovoltaic system with battery storage which is measured minute and hour basis solar irradiance data is studied. During overcast weather, there will be more fluctuation in the solar irradiance data due to the presence of clouds. McCormick and his team had simulated the results of the performance of a PV system in two different temporal resolutions. On 1st December 2012, they simulate the solar irradiance and current generated by the PV system in minute basis. The results are shown in Figure 10. The PV current is represented in negative values to indicate that it was supplied to charge the battery.

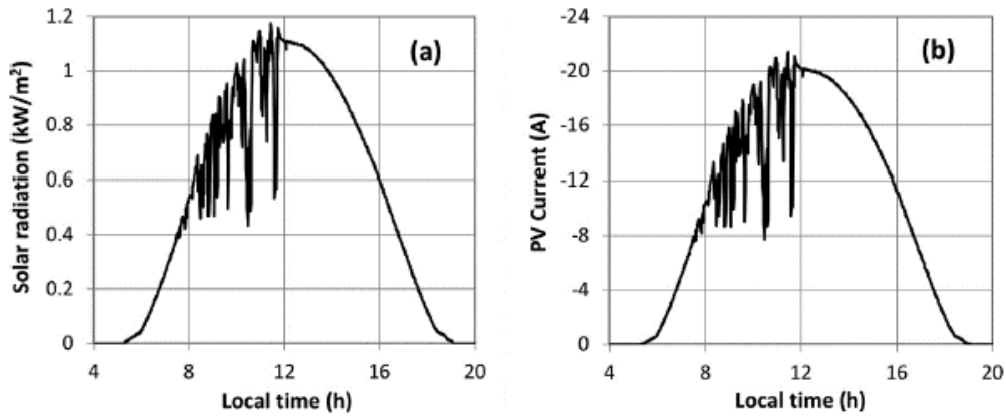


Figure 10: Simulated results of solar irradiance and PV current by McCormick. (McCormick and Suehrcke, 2018)

Figure 11 shows the changes in the current of the generator (I_{Gen}), PV (I_{PV}), battery (I_{Bat}), and load (I_{PVD}). Based on the graph plotted in Figure 11, in the early morning when there is no sunlight, the generator supplies current to the system. It slowly decreases until time is 8.2h. From morning to afternoon, the PV array will charge the battery and provide current to the loads. As can be observed from the graph, the fluctuation of solar irradiance causes the PV current to fluctuate too. Thus, the battery's charging current will also oscillate. After 11.6h, the fluctuation reduced. When the battery achieves the maximum state of charge (SOC_{max}), it will stop charging. At 15.7h, the PV current drops to less than the load current. Now, the battery supplies current to the loads until it reaches its maximum discharge current. After that, the generator will start to take over and the cycle continues.

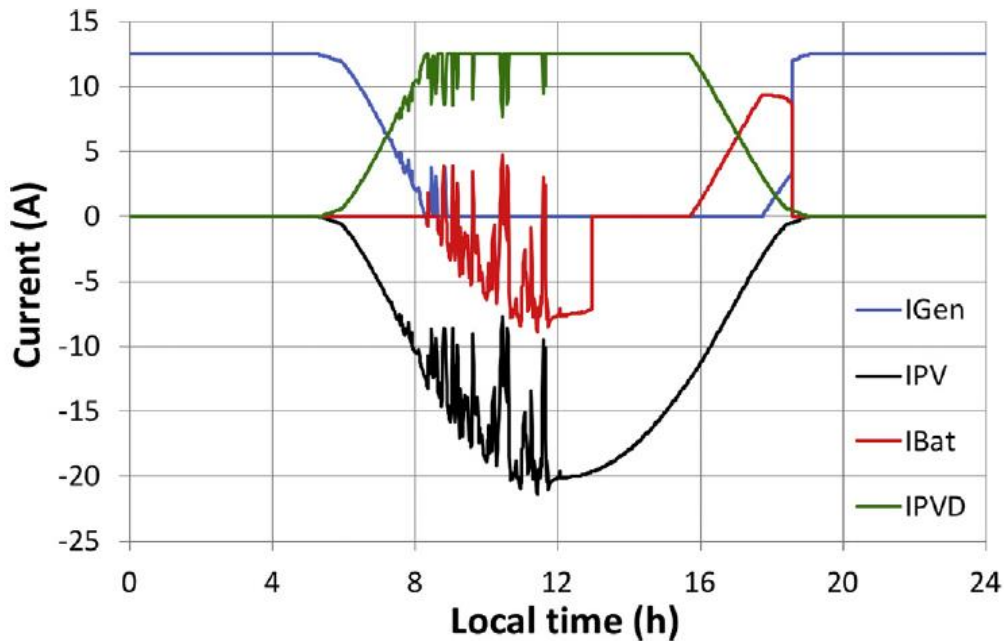


Figure 11: Graph of current from all devices vs the local time. (McCormick and Suehrcke, 2018)

Based on Figure 12, the fluctuation in solar irradiance and battery current cannot be observed in hourly data due to its low temporal resolution. Besides that, the total daily energy delivered by the system is also slightly higher in minute basis data compared to hourly data. Figure 13 shows that in hourly generated data, the state of charge (SOC), will rise until the maximum SOC is achieved. On the other hand, in the minute basis generated data, the battery never achieves maximum SOC. This is because the minute generated data will detect the presence of clouds within an hour. The presence of clouds causes the battery to discharge and thus lower the state of charge regularly.

Nowadays, more and more high temporal resolution solar irradiance measurement methods are used around the world. With a higher resolution measurement, it is more accurate to estimate the battery degradation rate and lifetime in a small PV system. (McCormick and Suehrcke, 2018)

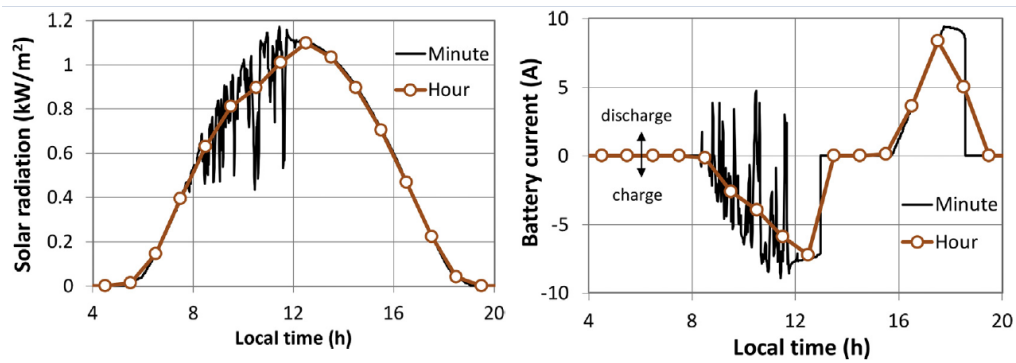


Figure 12: Graph of solar irradiance vs local time and graph of battery current vs local time in hour and minute basis. (McCormick and Suehrcke, 2018)

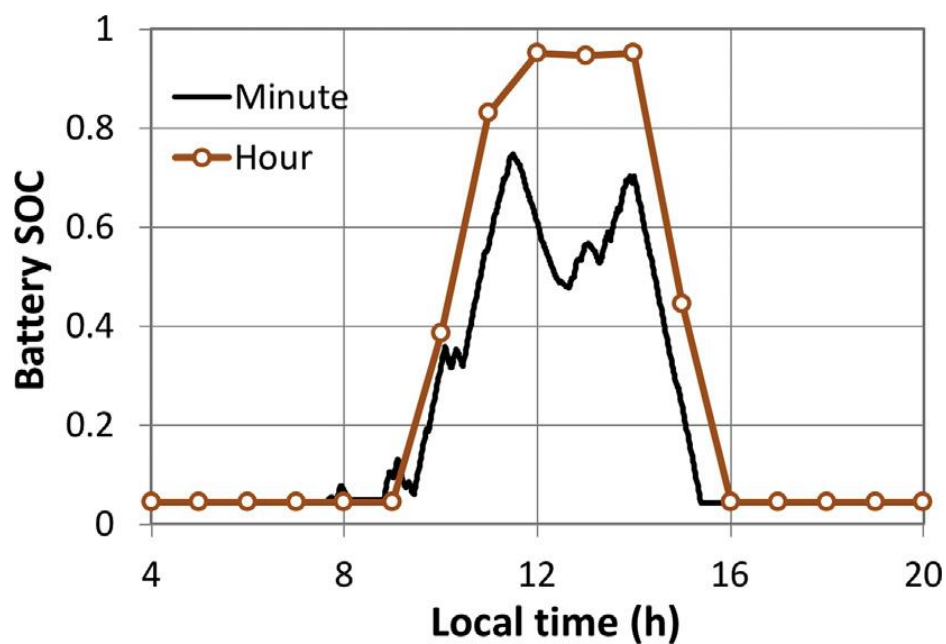


Figure 13: Graph of battery current vs local time in minute and hourly basis. (McCormick and Suehrcke, 2018)

2.2.8 The effect of compensation of photovoltaic systems with the grid to help to improve the voltage drop problem.

A study had been done in northern Algeria to solve the voltage drop problem that affects the living of residents in that area. A small photovoltaic site has been set up to compensate with the grid so that the voltage drop in the area will be lower than 10%. According to the graph plotted in Figure 14, the voltage drop had exceeded 10%.

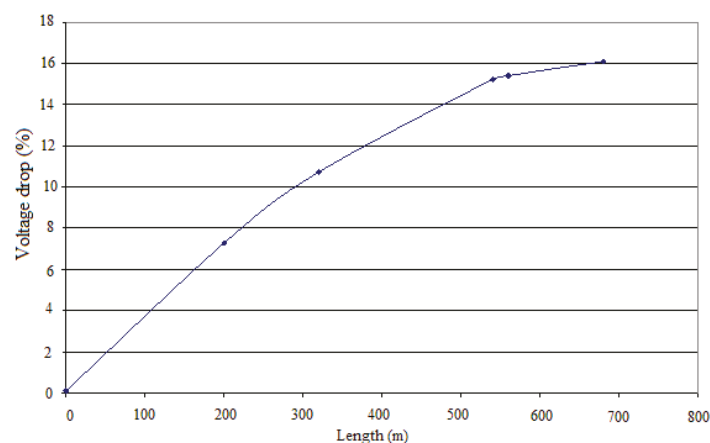


Figure 14: Graph of voltage drop vs the length of transmission line between transformer and load before installation of PV systems. (Mouheb, Hamidat, and Loukarfi, 2012)

From the study done by Mouheb, 10 sets of photovoltaic modules with a rating of 150 Wp, 24 V was installed into the grid. The mini photovoltaic systems were installed 300m away from the transformer. After installation, the voltage drop has a significant reduction as shown in Figure 15. Figure 15 shows voltage drops for different line lengths with and without the insertion of PV systems. The installation of PV systems helps to lower the voltage drop by decreasing the current flows through the line. Figure 16 shows the amount of current that flows through the line at different hours. This study proves that the compensation of PV systems to the grid can help to reduce the voltage drop in a low voltage network. (Mouheb, Hamidat, and Loukarfi, 2012)

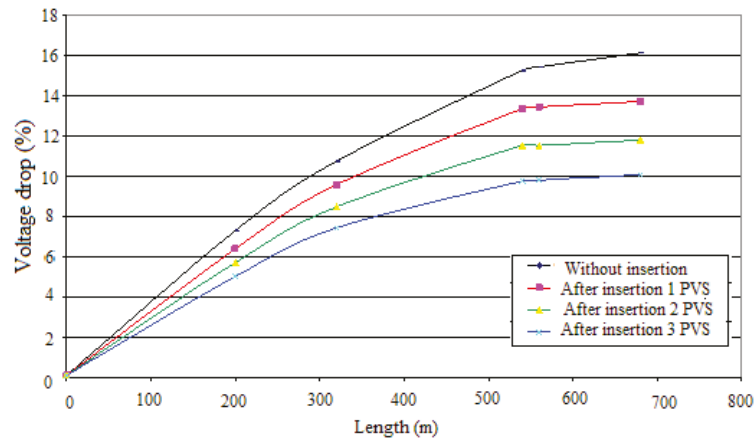


Figure 15: Graph of voltage drop vs the length of transmission line between transformer and load after installation of several PV systems. (Mouheb, Hamidat, and Loukarfi, 2012)

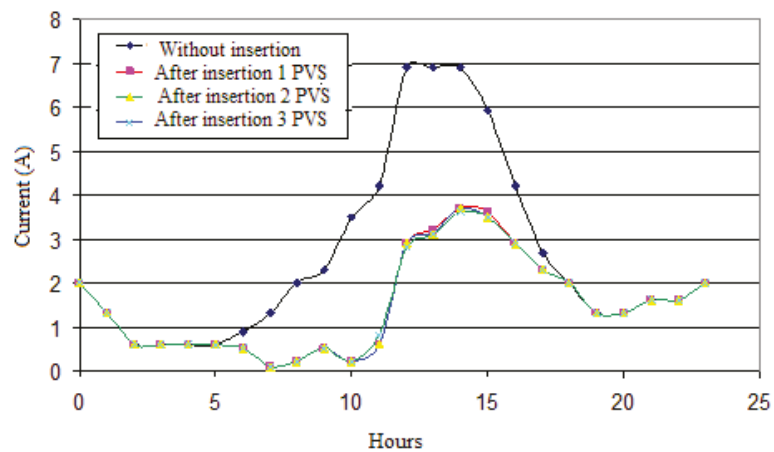


Figure 16: The effect on the current produced before and after the installation of PV systems. (Mouheb, Hamidat and Loukarfi, 2012)

CHAPTER 3

METHODOLOGY AND WORK PLAN

3.1 Overview

In this chapter, all the methods that are used to build the high-resolution temporal solar irradiance measurement system will be reviewed. The main idea of this project is to build a functional, reliable, and low-cost solar irradiance measurement system to collect solar irradiance data and compare it with the weather station.

Recently, most of the resolution of temporal solar irradiance is ranged between an hour to a month. Ramkumar set the sampling interval of one second during his research. (Jayaraman and Maskell, 2012). However, according to Chen and Brady, a higher cost may be needed for a larger amount of data when a higher resolution of 10 seconds or faster while sizing an inverter. (Chen and Brady, 2010). After considering these factors, a high-frequency sampling rate of 10 seconds is chosen to be implemented in this project by referring to a published paper written by Matthew Lave stating that the maximum percentage of error when applying 30-seconds sampling interval is only 3%. (Lave et al., 2017)

3.2 Overall circuit construction

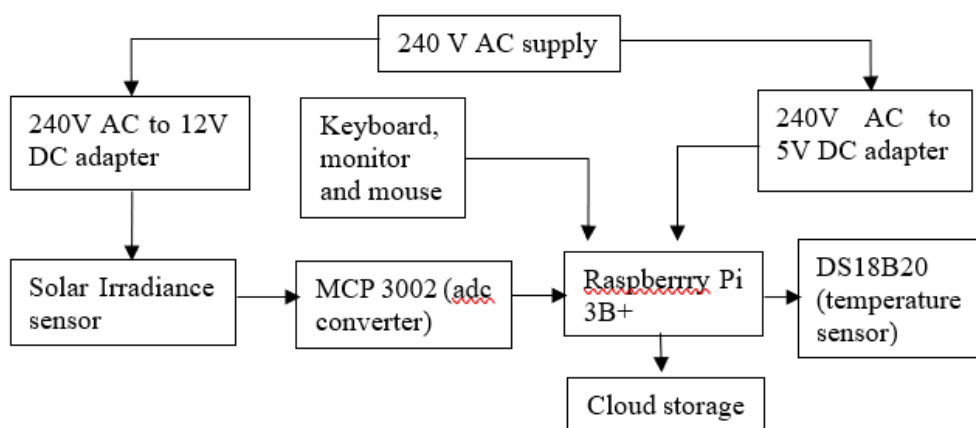


Figure 17: Block diagram of the whole circuit construction.

Figure 17 shows the interrelation between all the components in the system. First, the 240V AC power supply is used to power up the Raspberry Pi 3 B+ and SOZ-03 Silicon solar radiation analog sensor via the 240V AC to 5V DC adapter and 240V AC to 12V DC adapter. The solar irradiance meter then collects sunlight and sends a signal to Raspberry Pi. Since Raspberry Pi can only receive digital signals and the irradiance meter outputs analog signals, the signal is converted into digital form via MCP 3002 Analogue-to-Digital (ADC) converter. A DS18B20 temperature sensor is used to obtain a more accurate temperature reading and send it to Raspberry Pi. After gathering the temperature and solar irradiance data, a comma-separated value file is created inside Raspberry Pi and it is then be sent to cloud storage. A python program is written so that it will collect irradiance and temperature data every 10 seconds. The full circuit diagram of a system is shown in Figure 18.

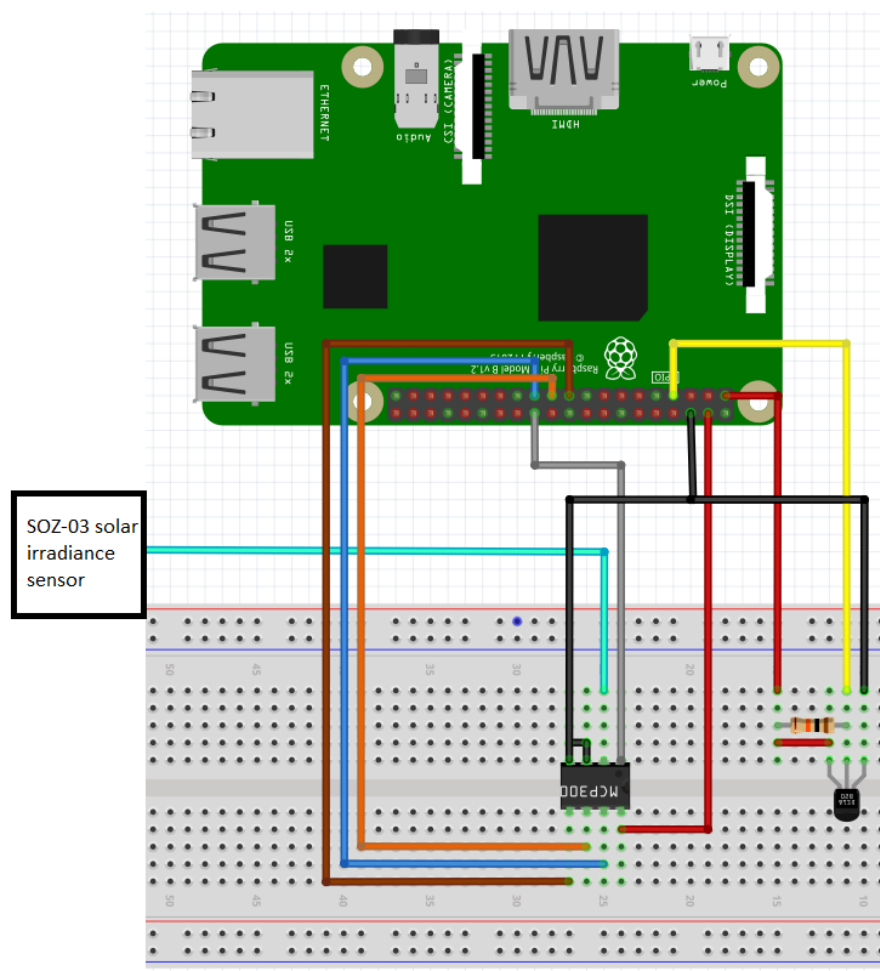


Figure 18: Circuit diagram

3.3 Raspberry Pi 3B+



Figure 19: Raspberry Pi 3B+

Figure 19 shows the image of a Raspberry Pi 3B+ model. This is the second latest model in the market. It has a built-in 1.4 GHz 64-bit quad-core processor, dual-band wireless LAN, Bluetooth 4.2/BLE. It also has four USB 2.0 ports, Gigabit Ethernet over USB 2.0, and a full-size HDMI port. (Raspberry Pi Foundation, 2016). The two common controller boards available are the Raspberry Pi and Arduino. Table 1 shows the main differences between Arduino and Raspberry Pi. According to Table 1, Raspberry Pi is found out to be more suitable as compared to Arduino. Since the solar irradiance data needed to be updated to the cloud storage frequently, built-in Wi-Fi connection ability is important. Besides that, Raspberry Pi as a single board computer, it is more reliable when handling a large amount of data. However, the main disadvantage of Raspberry Pi is it only can receive digital input instead of analog. Thus, MCP 3002 is needed to convert the output from the solar irradiance sensor into digital signals before feeding it to the microcomputer.

Table 1: Comparison between Arduino and Raspberry Pi(What are the differences between Raspberry Pi and Arduino?, 2017)

Raspberry Pi	Arduino
A single-board computer runs with Raspbian. It can perform multiple tasks at the same time	A microcontroller that can only run a program in a loop for a long time.
Need to install libraries online to communicate with sensors and devices	Easy to communicate with sensors and devices.
Higher cost	Lower cost
Can connect to the Internet via Wi-Fi or Ethernet port	Need an external module to connect to the Internet
Need a micro SD card for storage	Has storage onboard
Need to shut down to prevent software failure	Simple plug and play
Python as the main programming language	C++ as the main programming language
Consists of 4 USB port	Consists of only 1 USB port to communicate with a computer

3.4 Setting up Raspberry Pi

Since the Raspberry Pi is used as the microprocessor in this project, some setups needed to be done before programming it. First, the system should be booted up. In order to boot up the system, a micro SD card is required. In this project, a 32GB micro SD card is used. An operating system called Raspbian is downloaded from the official website and saved into the micro SD card. The micro SD card is then inserted into Raspberry Pi. Next, Raspberry Pi is powered up using a micro USB 240 V AC to 5 V DC converter. After powering up, it is connected to a monitor via HDMI to VGA converter. A keyboard and mouse are connected to the Raspberry Pi. Raspbian is installed into Raspberry Pi.


```

pi@raspberrypi: ~
a new password.

pi@raspberrypi:~ $ vncserver
VNC(R) Server 6.4.1 (r40826) ARMv6 (Mar 13 2019 16:35:06)
Copyright (C) 2002-2019 RealVNC Ltd.
RealVNC and VNC are trademarks of RealVNC Ltd and are protected by trademark
registrations and/or pending trademark applications in the European Union,
United States of America and other jurisdictions.
Protected by UK patent 2481870; US patent 8760366; EU patent 2652951.
See https://www.realvnc.com for information on VNC.
For third party acknowledgements see:
https://www.realvnc.com/docs/6/foss.html
OS: Raspbian GNU/Linux 10, Linux 4.19.50, armv7l

On some distributions (in particular Red Hat), you may get a better experience
by running vncserver-virtual in conjunction with the system Xorg server, rather
than the old version built-in to Xvnc. More desktop environments and
applications will likely be compatible. For more information on this alternative
implementation, please see: https://www.realvnc.com/doclink/kb-546

Running applications in /etc/vnc/xstartup

VNC Server catchphrase: "Vibrate button volume. Million Abraham good."
signature: a3-8c-ba-7a-d6-b1-b7-31

Log file is /home/pi/.vnc/raspberrypi:1.log
New desktop is raspberrypi:1 (192.168.0.19:1)
pi@raspberrypi:~ $ sudo get-update
sudo: get-update: command not found
pi@raspberrypi:~ $ sudo apt-get update

```

Figure 20: Command to update the Raspberry Pi

In order to update and upgrade the Raspberry Pi, “sudo apt-get update” and “sudo apt-get upgrade” commands are typed in the terminal. Figure 20 shows the command to update the Raspberry Pi. After updating and upgrading the system, Raspberry Pi Configuration needs to be configured. SPI, VNC, and SSH are enabled. SPI (Serial Peripheral Interface) is needed to communicate with the devices connected. VNC (Virtual Network Computing) is a graphical desktop-sharing system so that a computer can control another computer via the Internet. SSH (Secure Shell) is enabled in order to access to the remote machine and run commands. Both VNC and SSH are needed when we need to access to the raspberry pi using own laptop without monitor, mouse, and keyboard.

3.5 NES Silicon Solar Radiation Sensor Type SOZ-03



Figure 21: SOZ-03 Silicon Solar Radiation Sensor Type

The SOZ-03 Silicon Solar Radiation Sensor is the solar irradiance sensor used in this project. The reason this type of sensor is chosen is that it is smaller in size, made up of Monocrystalline Silicon cell, durable and stable, and is protected properly under a piece of laminated glass. The internal circuit is covered inside an excellent weatherproof junction box. (Viel, n.d.)

Table 2: Specification of SOZ-03 Silicon Solar Radiation Sensor

Linear output signal range	50 – 1500 W/m ²
Output signal voltage	90 – 110 mV
Integrated signal amplifier with output signal	4 – 20 mA Loop power two wires
Small drift	<0.3 % per year

3.6 DS18B20

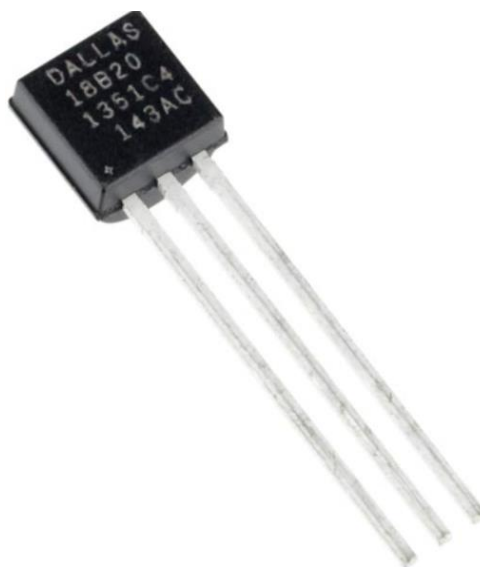


Figure 22: DS18B20

DS18B20 is a digital temperature sensor. DS18B20 is chosen because it is small, easy to configure, and has a more accurate measurement compared to other types of temperature sensors such as DHT 11. Other than that, DS18B20 is also suitable to be implemented in this project because it only outputs digital signals to the controller board. Raspberry Pi can only accept signals in digital form.

Table 3: Specification of DS18B20

Input voltage range	3.0 – 5.5 V
Storage temperature range	-55 - +125 °C
Thermometer error	± 2 °C
Typical current	1-1.5 mA

3.7 MCP3002

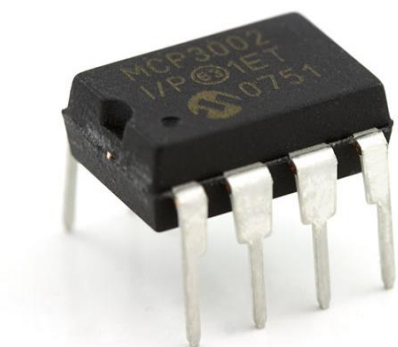


Figure 23: MCP 3002

MCP 3002 is a dual-channel 10-bits Analog-to-Digital Converter, ADC, Integrated Circuit (IC). MCP 3002 is used to convert the analog input from the SOZ-03 Silicon solar radiation analog sensor into digital form so that the signal can be interpreted in Raspberry Pi. It consists of two different input channels. In this project, the input channels are set to function as single-ended inputs. Standard Serial Peripheral Interface is configured to communicate between MCP 3002 and Raspberry Pi. (Microchip, 2008)

Table 4: Specification of MCP 3002

Input voltage range	2.7 – 5.5 V
V_{REF}	5.0 V
Industrial temperature range	-40 - +85 °C
Resolution	10 bits
Sampling frequency	200 ksps

3.8 Coding

After setting up Raspberry Pi, the next step is to install all the libraries which are needed. First, the library for the DS18B20 temperature sensor is installed by typing the command “sudo pip3 install w1thermsensor” in the terminal. The other thing that needed to be installed is the geocoder. It helps to verify the location of the sites. The command “sudo pip install geocoder” is typed in the terminal. Next, the libre office is installed to view the data collected in csv file format. It is similar to Microsoft Office in Windows. “sudo apt-get install libreoffice” needed to be typed in the terminal.

The complete coding named “KYedit5.2.2020.py” is attached in Appendix A. First, all the libraries which are needed to run the program are imported and defined. Next, the program will check for the year, month, and day in the “log” folder within the Raspberry Pi. If it does exist, then it will continue to run the next part, or else it will create a new folder named with the year and month. It will also create a new csv file with the headers of “location, Time, Temp, Voltage, Irradiance” if the file did not exist. After checking, the program will exit the file with the command “f.close”. The program will continue to define the current time. If the time is in every 10 seconds, it will continue to execute the next line. The next line will call another function named “sensor()”. This function will extract data from the SOZ-03 solar irradiance sensor and DS18B20 sensor. Then, it will open the csv file and store the data into it. This coding will continue to run without stopping if the Raspberry Pi is not turned off.

However, if power shortages happen, Raspberry Pi will be turned off and turned on again after the electricity supply recovers. Someone has to manually run the code again to collect data manually. To solve this issue, the “rc.local” file in the system is edited so that the coding will execute automatically during startup. First, within the terminal, “sudo nano /etc/rc.local” command is typed to edit the file. Next, before the last line of the code, which is “exit 0”, the command “sudo python /home/pi/KYedit5.2.2020.py &” is typed and the file is saved. The ampersand sign, “&”, has to be included in the command, or else the Raspberry Pi may not start up properly. (Five Ways to Run a Program On Your Raspberry Pi At Startup, 2020)

3.9 Method of Measurement

3.9.1 Method of collecting data

SOZ-03 Silicon solar radiation analog sensor is the device used to measure the solar irradiance. Raspberry Pi 3B+ is programmed to collect the solar irradiance data every 10 seconds and send the data to the cloud. These collected data will then compare with the weather station's database. If the results of the comparison are acceptable, another two similar circuits are built and results are calibrated and analyzed. Graphs are plotted with the data collected.

While constructing the first circuit, the solar irradiance sensor is placed on a flat surface to harvest the global horizontal irradiance on 12th floor of UTAR Sungai Long. The output from the sensor will then be transferred to the Raspberry Pi 3B+ for storing and analysis in a comma-separated value file. A circuit which is constructed to obtain the solar irradiance data and the surrounding temperature is shown in Figure 24. Figure 25 shows an example of a comma-separated value file that is created to record the irradiance and temperature data on 1st Dec 2019.

Next, another two sets of the same system are duplicated so that the total of three systems can be placed at three different sites for data collection and analysis. However, there are some problems encountered during the setup of this project. The first problem is the happening of Movement Control Operation (MCO) in Malaysia. On 18th March 2020, the Malaysia government had announced MCO due to the spreading of the Covid-19 virus. Hence, this had interrupted the progress of the project.

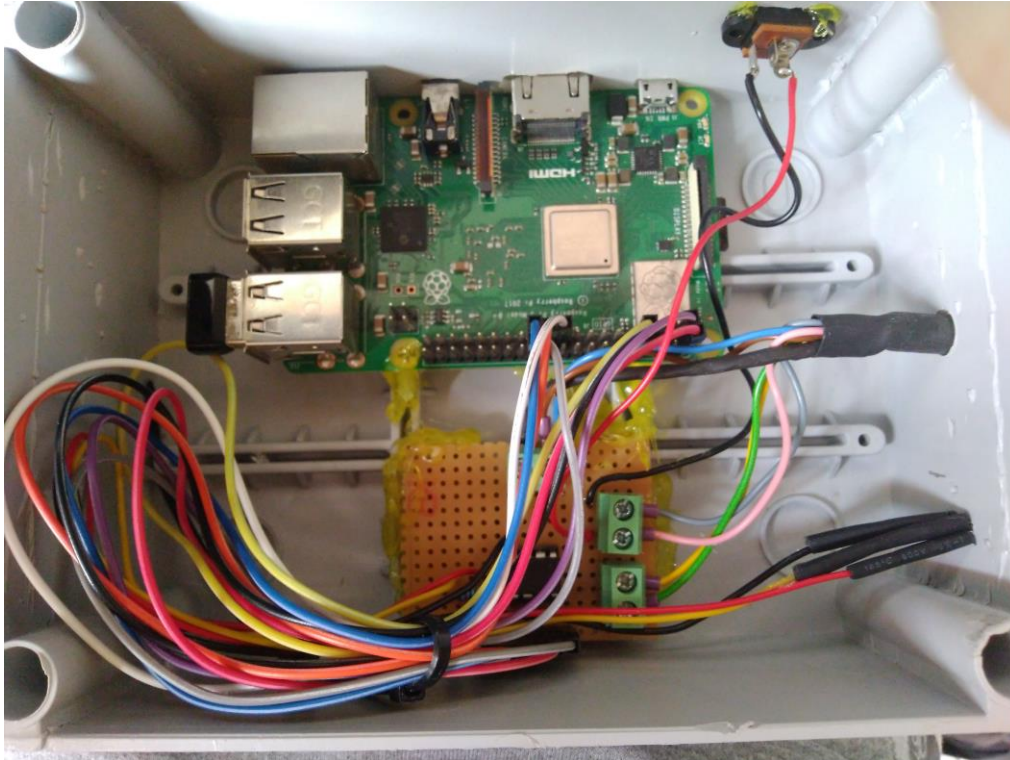


Figure 24: Circuit which is built for testing the functionality of MCP3002 and recording the surrounding temperature

	A	B	C	D	E	F	G	H	I	J	K	L	M
1	1/12/2019												
2	location	None											
3	Time	Temp	Voltage (mV)	Irradiance (W/m ²)									
4439	12:19:20	34.75	1660	398.4									
4440	12:19:30	34.687	1699	407.76									
4441	12:19:40	34.687	1674	401.76									
4442	12:19:50	34.625	1699	407.76									
4443	12:20:00	34.625	1684	404.16									
4444	12:20:10	34.562	1679	402.96									
4445	12:20:20	34.5	1689	405.36									
4446	12:20:30	34.5	1679	402.96									
4447	12:20:40	34.562	1694	406.56									
4448	12:20:50	34.562	1694	406.56									
4449	12:21:00	34.625	1708	409.92									
4450	12:21:10	34.562	1684	404.16									
4451	12:21:20	34.625	1694	406.56									
4452	12:21:30	34.75	1708	409.92									
4453	12:21:40	34.687	1738	417.12									
4454	12:21:50	34.687	1718	412.32									
4455	12:22:00	34.75	1718	412.32									
4456	12:22:10	34.812	1733	415.92									
4457	12:22:20	34.75	1743	418.32									
4458	12:22:30	34.812	1743	418.32									
4459	12:22:40	34.75	1757	421.68									
4460	12:22:50	34.812	1748	419.52									
4461	12:23:00	34.75	1767	424.08									
4462	12:23:10	34.75	1752	420.48									
4463	12:23:20	34.75	1757	421.68									
4464	12:23:30	34.812	1762	422.88									
4465	12:23:40	34.812	1767	424.08									
4466	12:23:50	34.75	1767	424.08									
4467	12:24:00	34.75	1767	424.08									
4468	12:24:10	34.75	1796	431.04									
4469	12:24:20	34.75	1796	431.04									

Figure 25: Comma-separated value file to record the irradiance and temperature data on 1st Dec 2019.

3.9.2 Method of Analysing data

Data from measurement resolution of 10-seconds, 1-minute, 5-minutes, and 30-minutes are extracted and study. 10-seconds resolution data is the original set of data from Raspberry Pi system. 1-minute resolution data are extracted from the 10-seconds resolution data by typing in the command “=AVERAGE(OFFSET(*the address of the first data from 10-seconds data*,(ROW()-ROW(*current row*))*6,,6))”. Value “6” in the command indicates that the data will be extracted every six rows in the 10-seconds resolution data. Next, for 5-minutes resolution’s data, a command “=AVERAGE(OFFSET(*the address of the first data from 10-seconds data*,(ROW()-ROW(*current row*))*30,,30))” is typed in. For a 30-minutes resolution’s data, a command “=AVERAGE(OFFSET(*the address of the first data from 10-seconds data*,(ROW()-ROW(*current row*))*180,,180))” is typed in the Excel sheet.

There are two methods for analyzing the data collected. The first method is to find out the standard deviation of the data. In order to calculate the standard deviation of different temporal resolution in Microsoft Excel, a command which is “=STDEV.P(IF(*range of data*<>0, *range of data*))” has to be typed in. In the command, the *range of data* means the range of cells that the standard deviation needed to be calculated. For example, if the data is stored in “H” column and from row “8” to row “4688”, thus the command is “=STDEV.P(IF(H8:H4688<>0, H8:H4688))”. Besides that, this command also will ignore all the cells in the range that contain “0” value.

Next, the second method is to find the difference of irradiance within data. For example, in 10-seconds resolution, the irradiance difference at 7:00:00 and 7:00:10 is calculated. “ABS(*data1* – *data2*)” command is input into Microsoft Excel. The *data1* and *data2* refer to the current irradiance data and subsequent irradiance data. The maximum irradiance difference is recorded and compared within different measurement time resolution. The results are shown in Chapter 4.

CHAPTER 4

RESULTS AND DISCUSSION

4.1 Comparison between Raspberry Pi data and Pyranometer's data

Solar irradiance data were collected at the rooftop of UTAR Sungai Long campus and were compared with the data collected by the pyranometer. Pyranometer collects data in minute basis while Raspberry Pi collects data in 10 seconds basis. Graphs are plotted in order to study the characteristic between both sets of data from pyranometer and Raspberry Pi.

4.1.1 Graph Comparison with the pyranometer

Three days in a month are shown in this section which are 1st Dec 2019, 15th Dec 2019, and 31st Dec 2019.

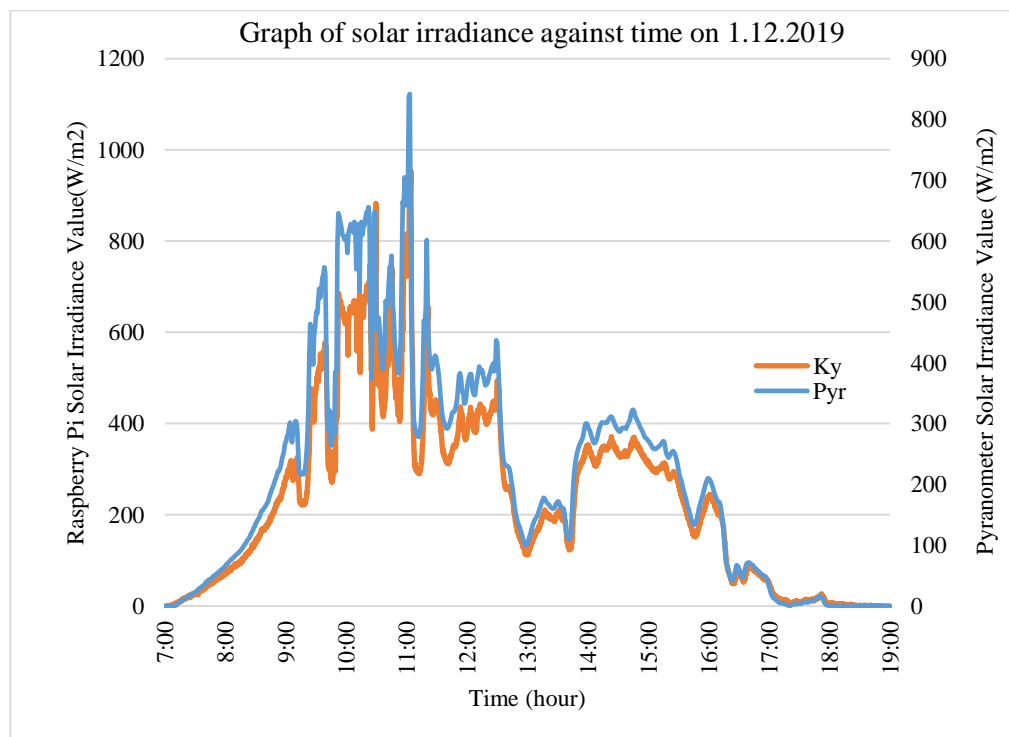


Figure 26: Comparison of data on 1.12.2019. Ky is the data collected by the Raspberry Pi circuit while Pyr is the data collected by the pyranometer.

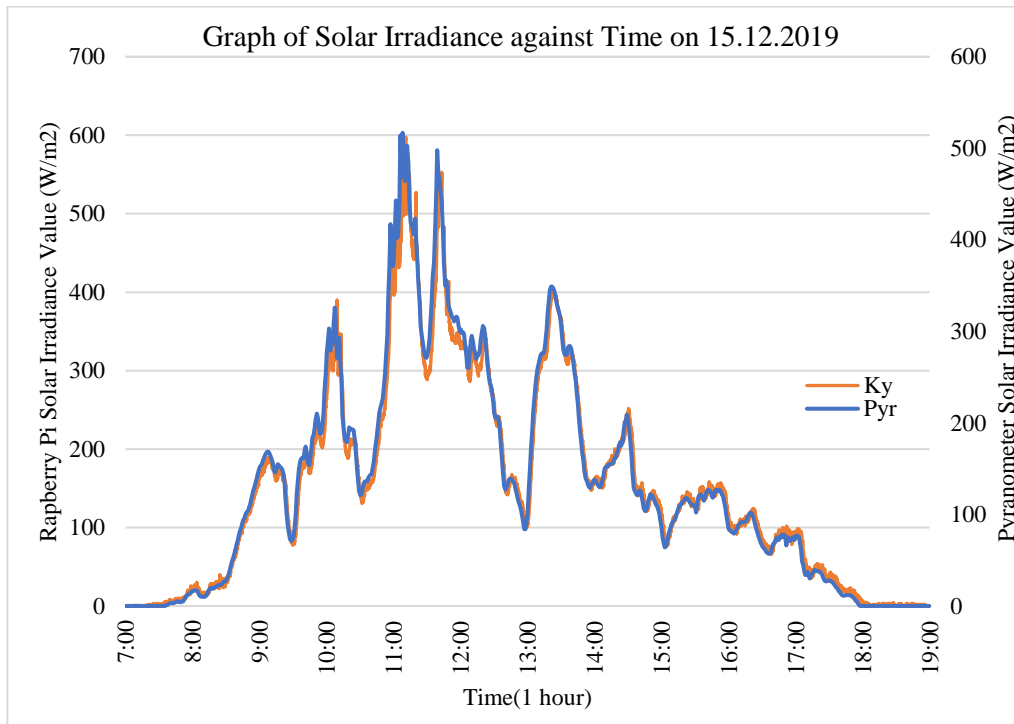


Figure 27: Comparison of data on 15.12.2019. Ky is the data collected by the Raspberry Pi circuit while Pyr is the data collected by the pyranometer.

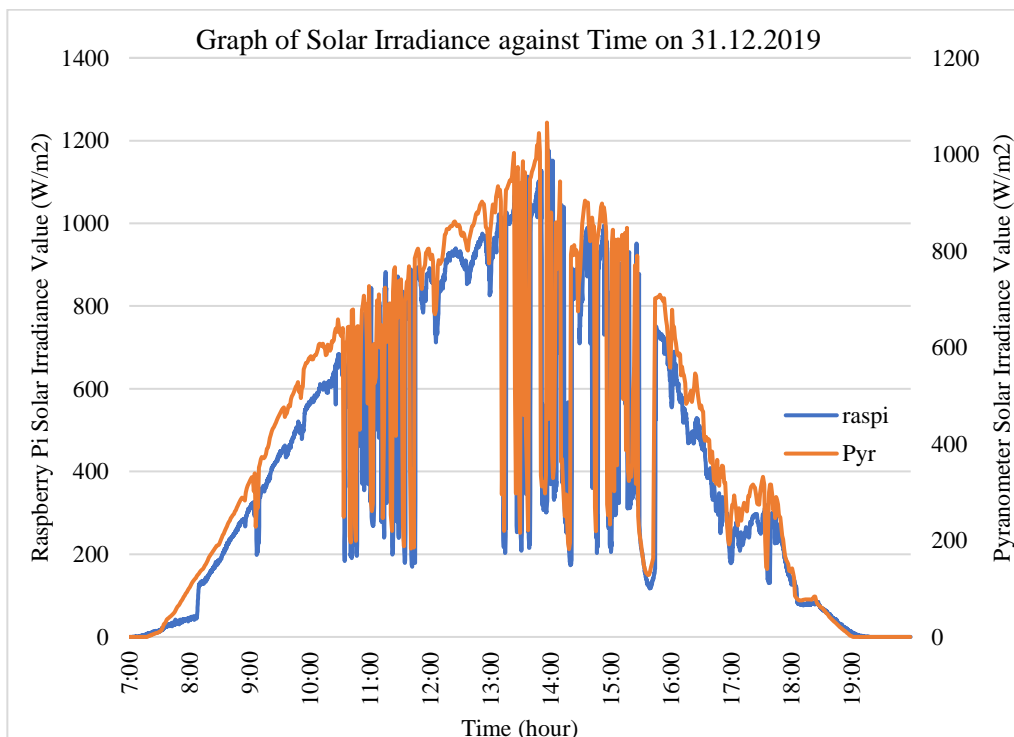


Figure 28: Comparison of data on 31.12.2019. Ky is the data collected by the Raspberry Pi circuit while Pyr is the data collected by the pyranometer.

The orange lines in the graphs of Figures 26, 27, and 28 show the result of the Raspberry Pi and SOZ-03 solar irradiance sensor with a resolution of 10 seconds while the blue line is the result of the pyranometer with the resolution of 1 minute. The primary y-axis at the left side of the graph represents the solar irradiance range for the pyranometer while the secondary y-axis at the right side of the graph represents the solar irradiance range for the SOZ-03 and Raspberry Pi.

Based on the results obtained in Figure 28, the trend for both temporal resolutions are almost similar. The difference between the two graphs is the graph with higher resolution will have more fluctuation compared to the graph with lower resolution. This fluctuation is useful while studying the intermittency of solar irradiance. Next, the results obtained from the Raspberry Pi and SOZ-03 irradiance sensor will have a higher solar irradiance reading. This may be due to the different types of measuring cells that are used to collect solar irradiance. In this project, a mono-crystalline measuring cell is used in the SOZ-03 solar irradiance sensor which is different from the one used in the pyranometer.

4.2 Data logging with the overGrive

OverGrive is an application that was developed by a website development company called The Fan Club. It is an application that can sync a computer to a Google Drive account. A new Gmail account will have a 15GB Google Drive storage. In this project, the solar irradiance data is uploaded to Google Drive using this method as long as the system is connected to the internet. Even though the internet is down for some technical issues, the data will automatically update to the cloud as soon as the network is fixed. Figure 29 shows a part of the data logged to the cloud. Once the data has been updated, it can be viewed anywhere and anytime. The cost of an overGrive account is RM21.59.

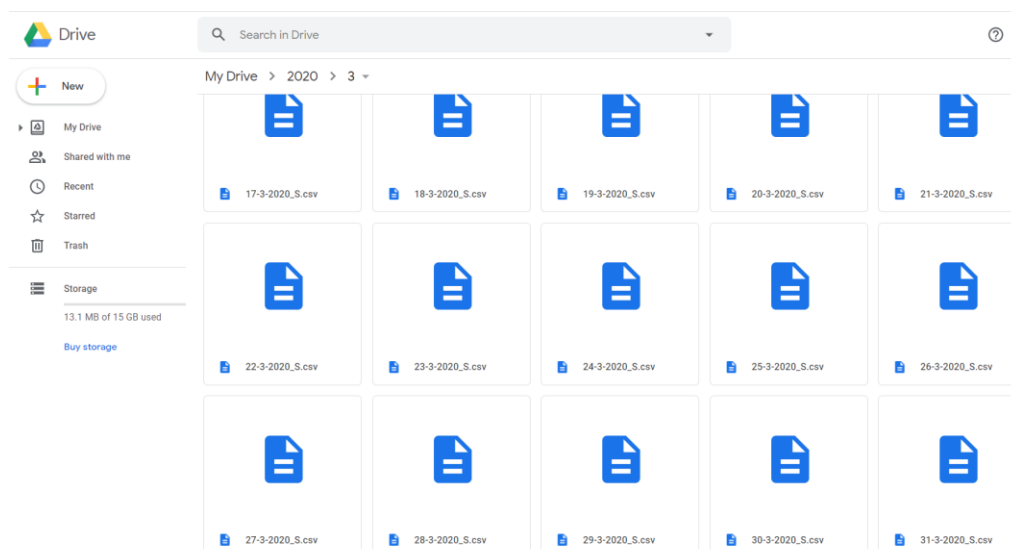


Figure 29: Solar irradiance data stored in Google Drive.

4.3 Duplicating of three sets of circuits.

After the results of the first set's data are compared with the pyranometer's data, another three sets of circuits are constructed. These three sets of circuit are calibrated. All these sets are labelled as Set 1, Set 2, Set 3, and Set 4. However, Set 4 project was abandoned in this project due to the insufficient of Raspberry Pi as the cost of purchasing is quite high. Moreover, the happening of MCO is also one of the causes.

First, Set 1 and Set 2 are compared. After comparing the results, both circuits' data are similar and are shown in Figure 30. Besides that, the percentage difference between the first set and the second set is also calculated. It is calculated using formula (2). In Equation (2), D_1 represents data from the first set, while D_2 represents data from the second set. D_{ave} is the average data from the first and second set. The percentage difference between these two sets of data was shown in Figure 31. Based on the graph, from 8:30:00 to 18:00:00, the percentage difference between these two sets is around 1.5%.

$$\frac{|D_1 - D_2|}{D_{ave}} \times 100\% \quad (2)$$

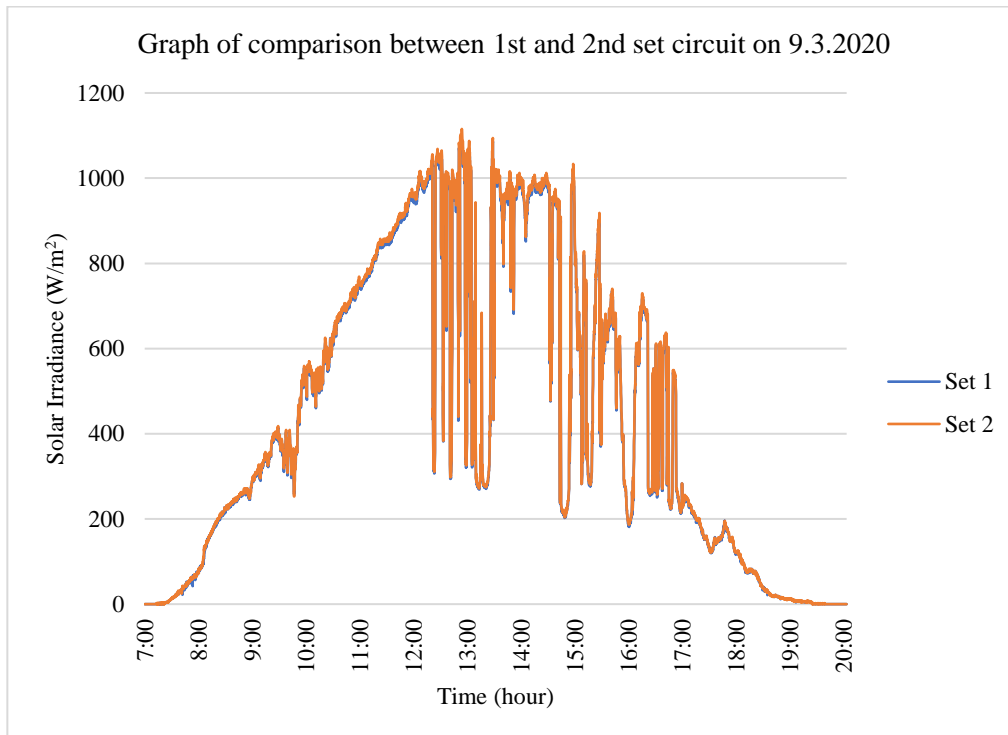


Figure 30: Graph comparison between the first set and the second set circuit. The blue line represents set 1 while the orange line represents set 2.

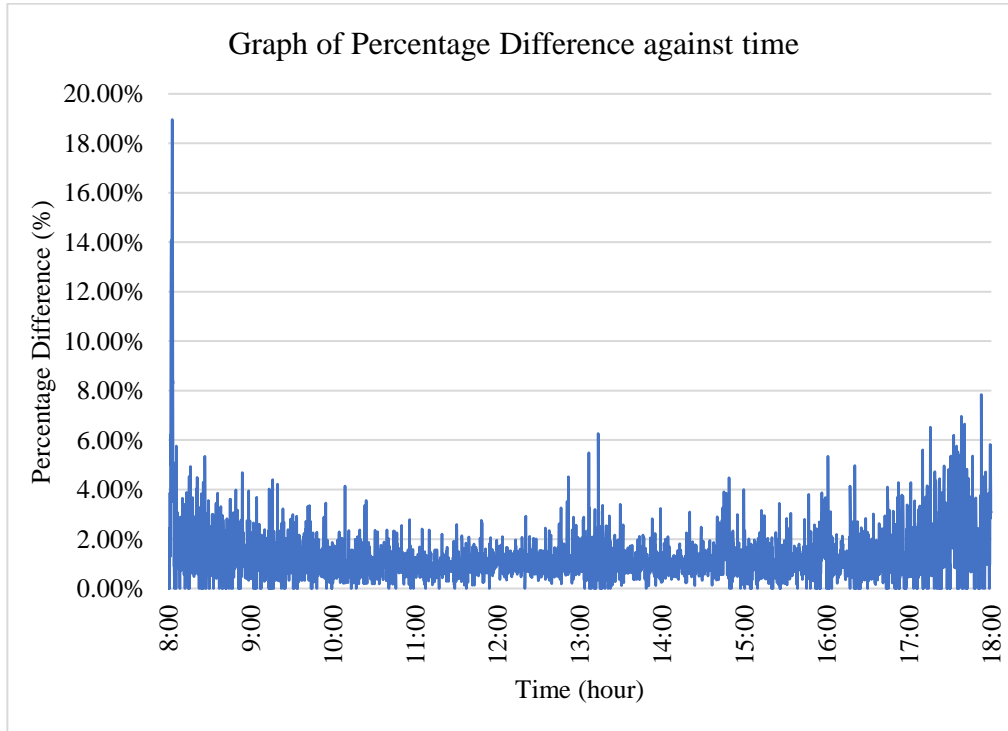


Figure 31: Percentage difference between the first and the second circuit from 8:00 to 18:00 on 9.3.2020.

Next, while calibrating Set 3, Set 2 is set as reference. The reason why this calibration of the three sets is carried out one by one is because of the limited space for the setup and lack of extension cord. The collected irradiance results are shown in Figure 32. The percentage difference was also calculated and shown in Figure 33. The percentage difference from 8:00 to 18:00 fluctuates at around 5%. This percentage difference may be caused by the offset error of the third set electronics part. Thus, the calibration of the third has to adjusted more before placing then system to the sites.

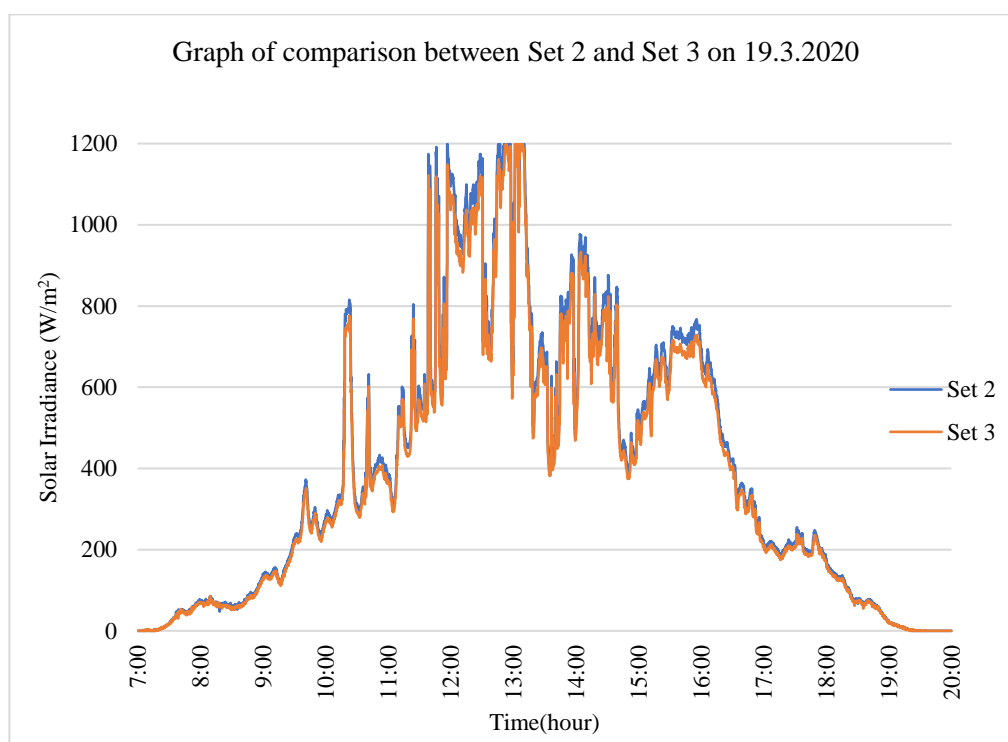


Figure 32: Graph of comparison between Set 2 and Set 3 on 19.3.2020. The blue line represents Set 2 while the orange line represents Set 3.

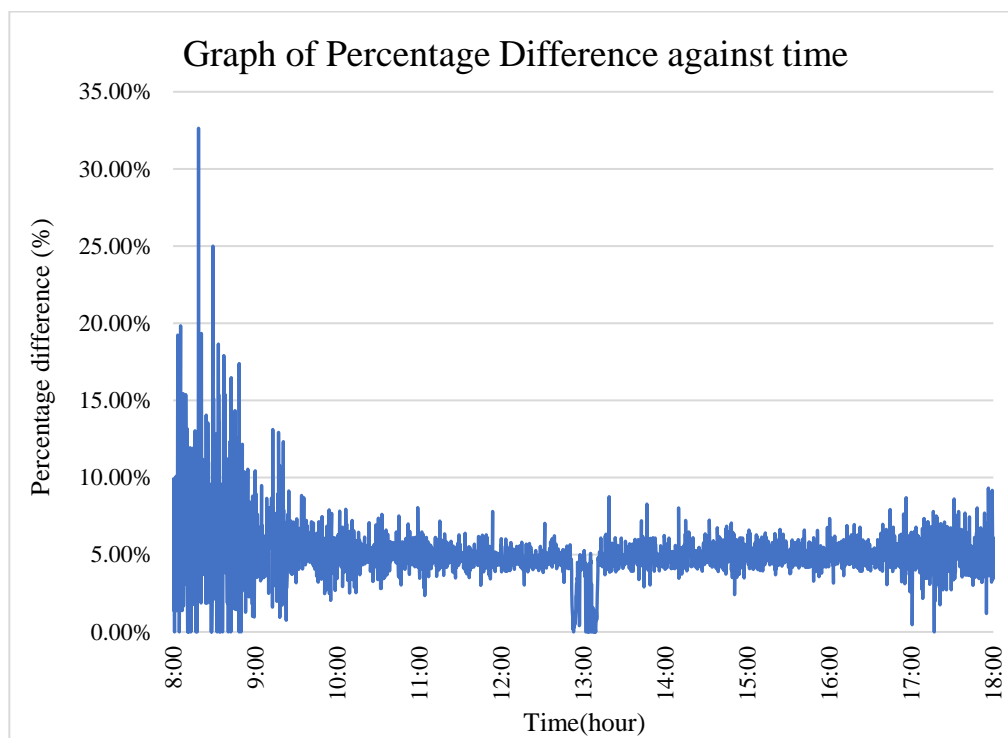


Figure 33: Percentage difference of second and third circuit from 8:00 to 18:00 on 19.3.2020

4.4 Analyzing the collected data from Set 2 comparing to different time resolutions.

After setting up the three sets of systems, initially, the plan was going to locate the system to three different sites for collecting data for solar irradiance intermittency study. However, due to the Movement Control Order (MCO) announced by the Malaysia government, the plan had to be cancelled. Thus, this part will discuss the analysis of data. The data is download from Google Drive for analysis purposes. In this section, only set 2's solar irradiance data is analyzed.

First, the graph for each temporal resolution is plotted to observe the frequency of high peak changes during the whole day. This study is to prove that whether a higher temporal resolution system can capture more peak changes and irradiance drop. The 1-minute, 5-minutes, and 30-minutes data are extracted from the original 10 seconds resolution system based on the method shown in 3.9.2. The results are shown in Figure 34, 35, and 36. Based on Figure 34, there are small differences between 10 seconds and 1-minute data. However, in Figure 35, it is evident that a 5-minutes system was unable to capture some peak

changes compared to 10 seconds system. The 30-minutes system's data is worse than a 5-minutes system. Thus, a higher temporal resolution measurement system should be implemented in a PV's industry especially when studying the intermittency of solar irradiance.

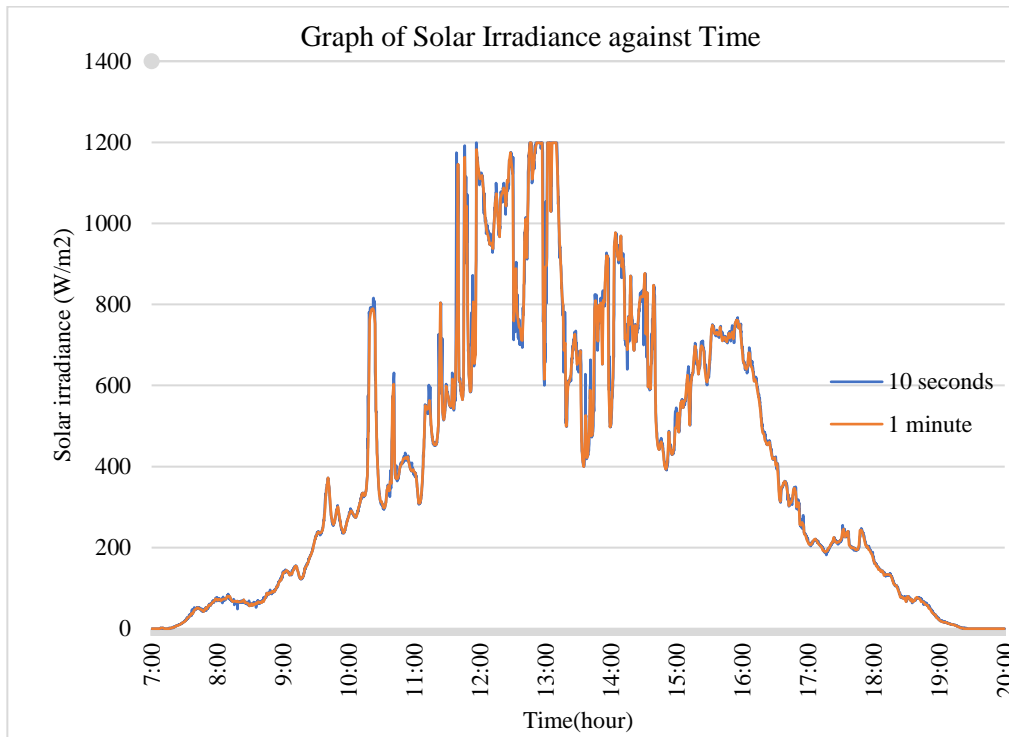


Figure 34: Graph of comparison between 10-seconds data with 1-minute data.

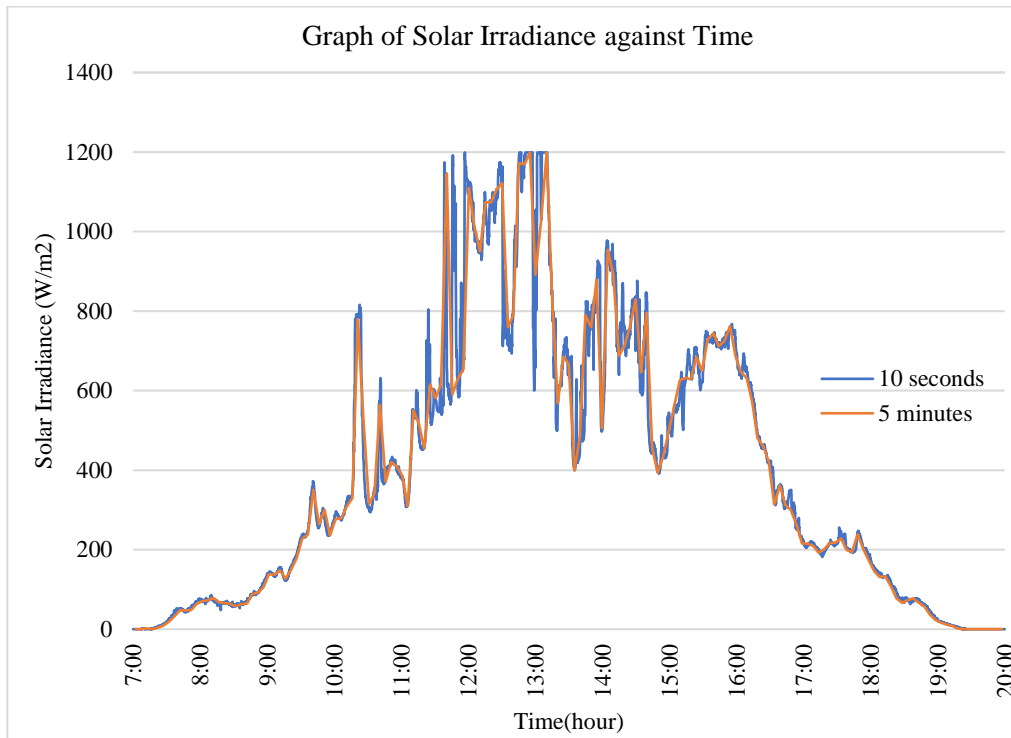


Figure 35: Graph of comparison between 10-seconds data with 5-minutes data.

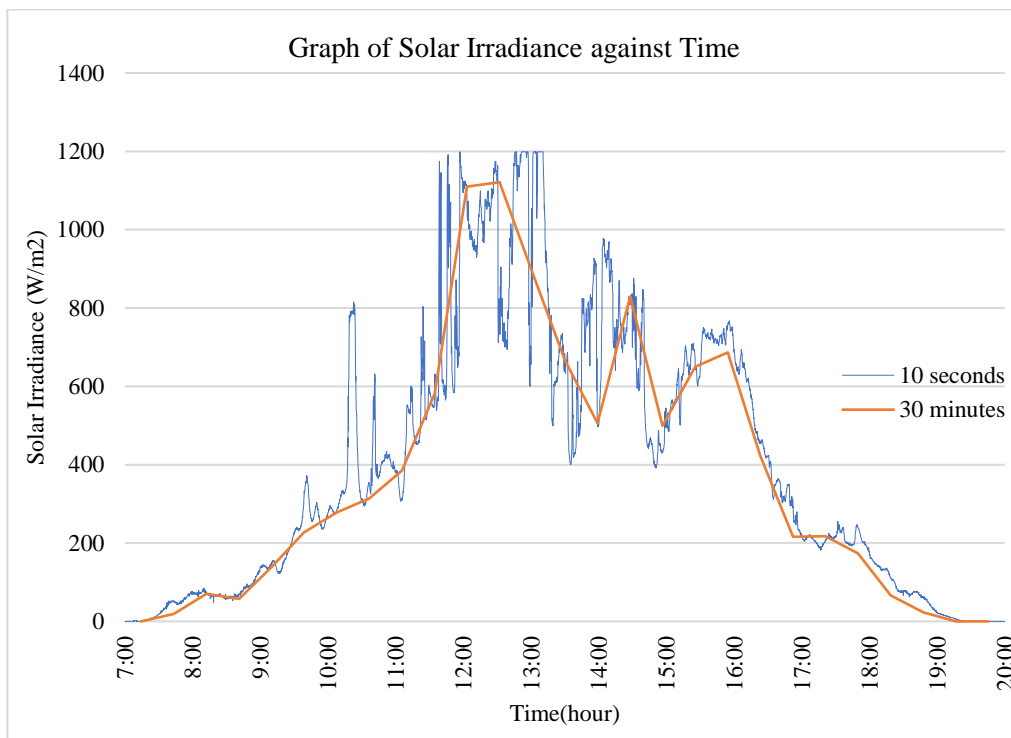


Figure 36: Graph of comparison between 10-seconds data with 30-minutes data.

Next, the standard deviation of different temporal resolution and maximum difference between points is calculated and the results are shown in Figures 37 and 38. The method of calculating standard deviation and maximum differences between points is shown in sub-chapter **3.9.2**. Based on the graph in Figure 37, it shows that within 15 days, the standard deviation of a higher resolution system is higher. This could be because of the amount of data collected. Since a higher resolution measurement system collects more data per day, the data will be more spread out from the mean irradiance, and thus, it will have a higher standard deviation.

Other than that, in Figure 38, the standard deviation of changes in solar irradiance is higher in the lower resolution system. This is because in a lower resolution system, the data collected is less. Thus, the frequency of high solar irradiance changes is higher compared to a higher resolution measurement system. This proves that the higher resolution measurement system can capture more data with higher accuracy.

Besides that, according to Figure 39, it is observed that most of the day, the maximum difference between points for a higher resolution system is lesser. The graph in the figure excludes the analysis for 30-minutes data because the 30 minutes resolution is too low compared to the others. This is again due to the number of data collected. More data indicates that the time interval between the two collected data is shorter. Within a shorter time-interval, the solar irradiance difference between two points is smaller.

Lastly, Figure 40 shows that the frequency of solar irradiance changes that is higher than 100 W/m^2 against the different time resolution measurement system. According to the line graph, the higher the resolution of solar irradiance measurement, the higher is the frequency of solar irradiance changes that is higher than 100 W/m^2 . This is because in a higher resolution system, more data is collected. Thus, more changes of solar irradiance can be tracked and analysed.

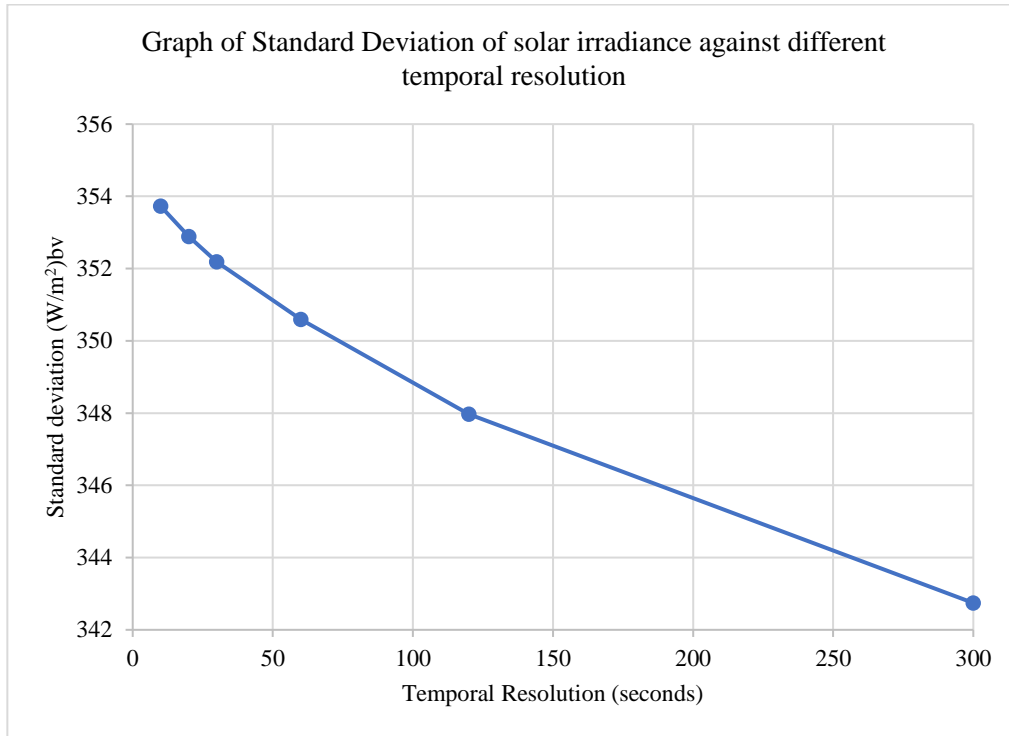


Figure 37: Graph of standard deviation against time resolution for 15 days. The time resolutions are 10-seconds, 20-seconds, 30-seconds, 1 minute, 2 minutes, and 5 minutes.

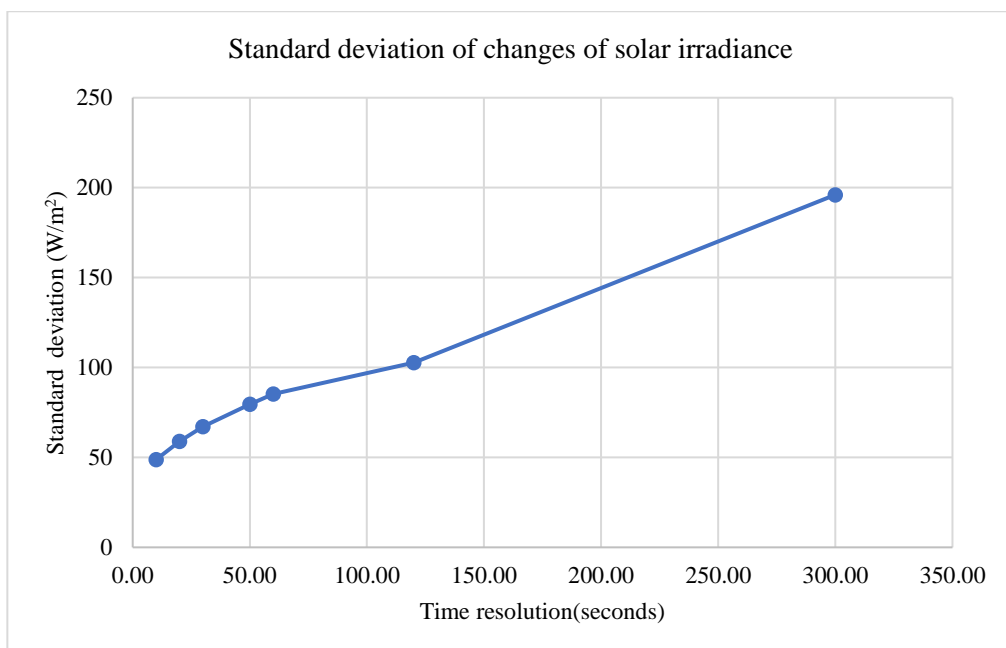


Figure 38: Graph of the standard deviation of changes in solar irradiance. The time resolutions are 10-seconds, 20-seconds, 30-seconds, 50-seconds, 1 minute, 2 minutes, and 5 minutes.

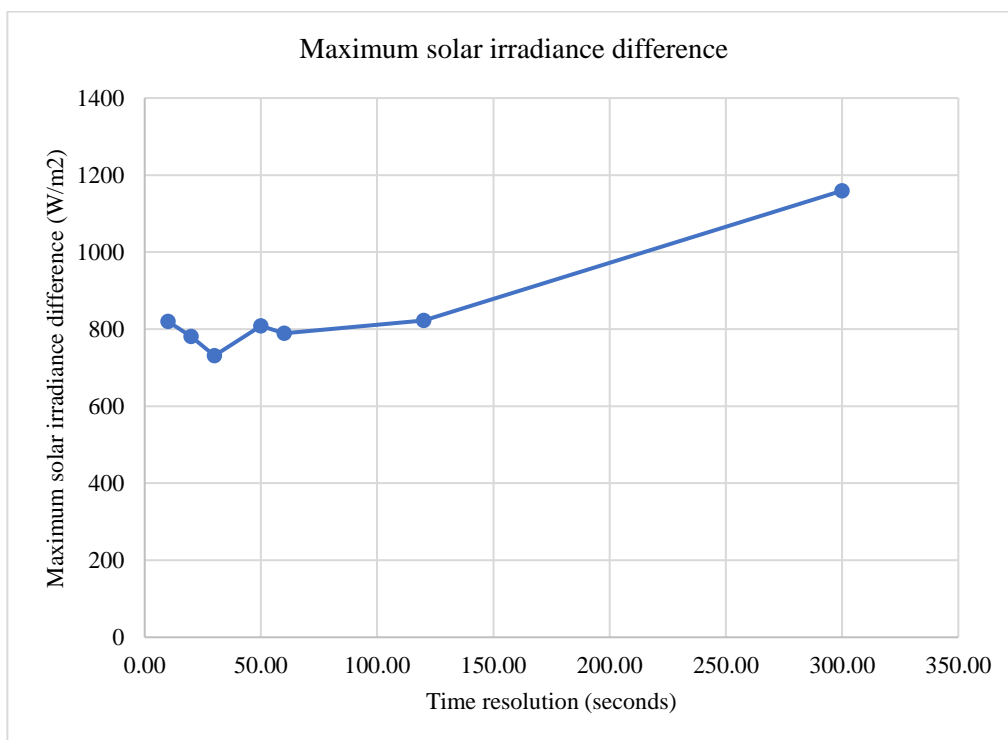


Figure 39: Graph of maximum solar irradiance difference between points against date. It compares between 10 seconds, 20 seconds, 30 seconds, 50 seconds, 1 minute, 2 minutes, and 5 minutes.

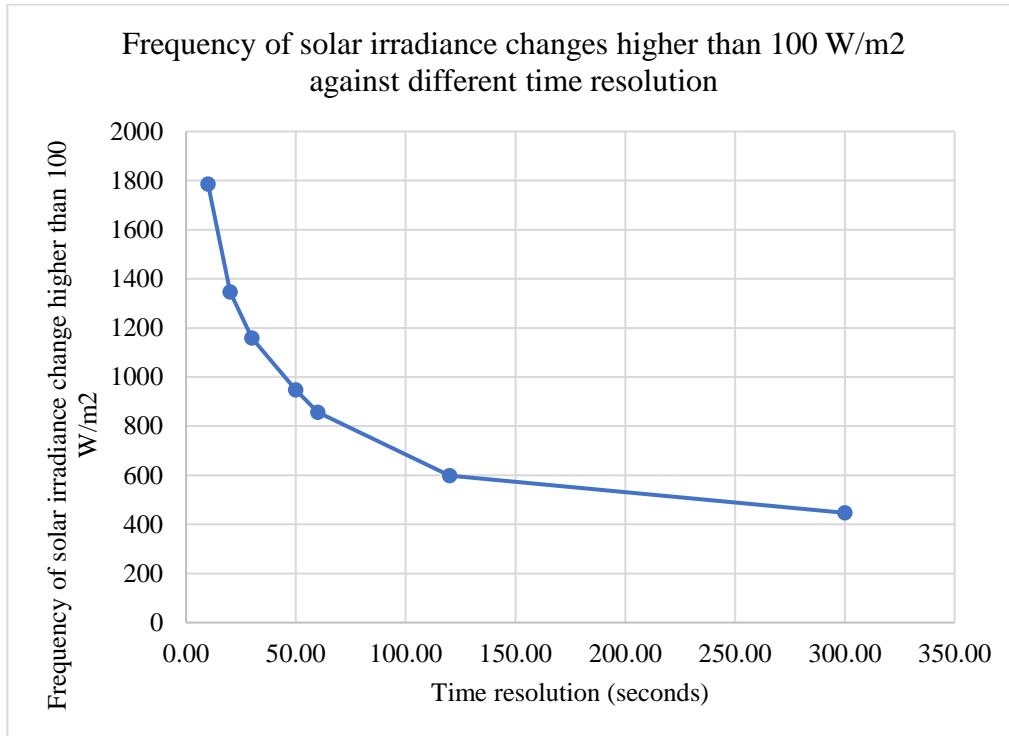


Figure 40: Graph of frequency of solar irradiance changes that is higher than 100 W/m² against different time resolutions. It compares between 10 seconds, 20 seconds, 30 seconds, 50 seconds, 1 minute, 2 minutes, and 5 minutes.

CHAPTER 5

CONCLUSION AND RECOMMENDATION

5.1 Conclusion

After analyzing the data, it can be concluded that a higher resolution temporal solar irradiance of 10 seconds should be implemented in the study of intermittency of solar irradiance. Besides that, the output from the SOZ-03 irradiance sensor and the output from the pyranometer will have a difference that fluctuates around 50% from 7:11 am to 5:03 pm. This may be due to the different materials used as solar irradiance sensors.

Next, the difference between each circuit constructed was compared for calibration purposes. According to the results, the percentage difference between the first and the second circuit is smaller than 5%. The percentage difference between the second and the third circuit is within 5% to 10%. Thus, the calibration of the third circuit has to be improved. Other than that, the trend of the graph for 10seconds, 1 minute, 5 minutes, and 30 minutes resolution are observed and studied. It is concluded that 10 seconds resolution measurement system can capture the intermittency easier when compared to other time resolution measurement.

Besides that, according to the results plotted in Figure 38, 39, and 40, it proves that when more data is collected, more changes of solar irradiance can be tracked. The drop of solar irradiance will cause voltage drop if the solar PV system is connected to a grid. It is very helpful in the study of intermittency of solar irradiance. Furthermore, mutual compensation between a few different sites can also be studied once the intermittency is observed.

The main advantage of this system is the internet connectivity. This is due to the built-in Wi-Fi function in the Raspberry Pi. Therefore, the system can send the solar irradiance data to the cloud easily with Wi-Fi connection while the user can access the data anytime and anywhere. Moreover, the cost to build this system is cheaper compared to other solar irradiance sensor systems with a data logger.

After finishing this project, the three objectives had been met. Skills to build a simple yet reliable high temporal resolution solar irradiance measurement system is learnt. Other than that, the knowledge and characteristics of the solar irradiance are studied.

5.2 Future improvement

Initially, the project was planned to set up three same systems at different sites to study the intermittency of solar irradiance. However, the plan is unable to continue due to the MCO. Thus, it shall be improved after the MCO. More circuit can be built and placed around Malaysia to continue the study of intermittency of solar irradiance. Next, the mutual compensation between every site can also be implemented and studied in the future. Mutual compensation can be defined as the average of the solar irradiance data at 2 or more sites to solve the problems caused by the intermittency.

Next, in the future, the percentage difference between each system shall also be reduced to as low as possible. By doing this, all of the measurement systems can have a more precise reading. Other than that, a Wi-Fi USB modem can also be implemented into the system so that it can access the internet anytime. Besides that, the circuit for data collection can be designed and printed on a PCB board so that the connection inside the junction box can be more arranged.

REFERENCES

- Anon 2017. *What are the differences between Raspberry Pi and Arduino?* [online] Available at: <<https://www.electronicshub.org/raspberry-pi-vs-arduino/>> [Accessed 22 Aug. 2019].
- Anon 2019. *Solargis global solar radiation data / Time Series and TMY / Tech Specs / Solargis.* [online] Available at: <<https://solargis.com/products/evaluate/tech-specs>> [Accessed 24 Aug. 2019].
- Anon 2020. *Five Ways to Run a Program On Your Raspberry Pi At Startup.* [online] Available at: <<https://www.dexterindustries.com/howto/run-a-program-on-your-raspberry-pi-at-startup/>> [Accessed 16 Apr. 2020].
- Beyer, H.G., Decker, B., Luther, J. and Steinberger-willms, R., 1991. 1 \ 0.4.
- Blanc, P., Espinar, B., Geuder, N., Gueymard, C., Meyer, R., Pitz-Paal, R., Reinhardt, B., Renné, D., Sengupta, M., Wald, L. and Wilbert, S., 2014. *Direct normal irradiance related definitions and applications: The circumsolar issue.* *Solar Energy*, .
- Chen, S. and Brady, D., 2010. The Impact of Irradiance Time Behaviors on Inverter Sizing and Design. *2010 IEEE 12th Workshop on Control and Modeling for Power Electronics (COMPEL)*, (1), pp.1–5.
- Gueymard, C.A. and Wilcox, S.M., 2009. Spatial and temporal variability in the solar resource: Assessing the value of short-term measurements at potential solar power plant sites. *38th ASES National Solar Conference 2009, SOLAR 2009*, 5(June), pp.3026–3053.
- Hejase, H.A.N. and Assi, A.H., 2016. Estimation of Global and Diffuse Horizontal Irradiance in Abu Dhabi, United Arab Emirates. *Renewable Energy in the Service of Mankind Vol II*, (August), pp.3–14.
- Hontoria, L., Rus-Casas, C., Aguilar, J.D. and Hernandez, J.C., 2019. An improved method for obtaining solar irradiation data at temporal high-resolution. *Sustainability (Switzerland)*, 11(19).
- Jayaraman, R. and Maskell, D.L., 2012. Temporal and spatial variations of the

solar radiation observed in Singapore. *Energy Procedia*, 25, pp.108–117.

Lai, K., n.d. Comparative Study for Time-specific Ross Coefficient and Overall Ross Coefficient for Estimation of Photovoltaic Module Temperature.

Lave, M., Quiroz, J., Reno, M.J. and Broderick, R.J., 2017. High temporal resolution load variability compared to PV variability. *2017 IEEE 44th Photovoltaic Specialist Conference, PVSC 2017*, pp.1–6.

Lave, M., Reno, M.J. and Broderick, R.J., 2015. Characterizing local high-frequency solar variability and its impact to distribution studies. *Solar Energy*, 118, pp.327–337.

Lave, M. and Weekley, A., 2017. Comparison of high-frequency solar irradiance: Ground measured vs. satellite-derived. *2017 IEEE 44th Photovoltaic Specialist Conference, PVSC 2017*, pp.1–6.

McCormick, P.G. and Suehrcke, H., 2018. The effect of intermittent solar radiation on the performance of PV systems. *Solar Energy*, [online] 171(February), pp.667–674. Available at: <<https://doi.org/10.1016/j.solener.2018.06.043>>.

Mekhilef, S., Safari, A., Mustaffa, W.E.S., Saidur, R., Omar, R. and Younis, M.A.A., 2012. *Solar energy in Malaysia: Current state and prospects. Renewable and Sustainable Energy Reviews*, .

Microchip, 2008. MCP3004/MCP3008 datasheet. pp.1–40.

Mouheb, M., Hamidat, A. and Loukarfi, L., 2012. Impact of PV compensation in improving the voltage drop in electrical networks LV. *Energy Procedia*, 18, pp.751–761.

Musanga, L.M., Barasa, W.H. and Maxwell, M., 2018. The Effect of Irradiance and Temperature on the Performance of Monocrystalline Silicon Solar Module in Kakamega. *Physical Science International Journal*, 19(4), pp.1–9.

Patsalides, M., Evagorou, D., Makrides, G., Achillides, Z., Georghiou, G.E., Stavrou, A., Efthymiou, V., Zinsser, B., Schmitt, W. and Werner, J.H., 2007. The effect of Solar irradiance on the power quality behaviour of grid connected

photovoltaic systems. *Renewable Energy and Power Quality Journal*, 1(05), pp.323–330.

Perez, R., David, M., Hoff, T.E., Jamaly, M., Kivalov, S., Kleissl, J., Lauret, P. and Perez, M., 2016. Spatial and Temporal Variability of Solar Energy. *Foundations and Trends® in Renewable Energy*, 1(1), pp.1–44.

Raspberry Pi Foundation, 2016. Raspberry Pi 3 Model B. *Raspberry Pi Website*, [online] p.2837. Available at: <www.raspberrypi.org/products/raspberry> [Accessed 22 Aug. 2019].

Rathod, A.P.S., Mittal, P. and Kumar, B., 2017. Analysis of factors affecting the solar radiation received by any region. *2016 International Conference on Emerging Trends in Communication Technologies, ETCT 2016*, pp.1–4.

Sharma, D.P., Samuel, K., Ramoutar, K., Lowe, T. and David, I., 2017. Raspberry Pi Based Real Time Data Acquisition Node for Environmental Data Collection. *International Journal of Recent Trends in Engineering and Research*, (June), pp.293–299.

Singh, G.K., 2013. Solar power generation by PV (photovoltaic) technology: A review. *Energy*, 53, pp.1–13.

Viel, D.-G.L., n.d. *NES Mess-und Meldesysteme Measuring Systems Silicon Solar Radiation Sensor Type SOZ-03*.

Vindel, J.M. and Polo, J., 2014. Intermittency and variability of daily solar irradiation. *Atmospheric Research*, [online] 143, pp.313–327. Available at: <<http://dx.doi.org/10.1016/j.atmosres.2014.03.001>>.

APPENDIX

Appendix A: 10 seconds solar irradiance measurement system coding named “KYedit5.2.2020.py”

```
import time
import os
import geocoder
from datetime import datetime
from w1thermsensor import W1ThermSensor
import RPi.GPIO as GPIO
import spidev

spi = spidev.SpiDev()
spi.open(0, 0)
spi.max_speed_hz = 250000

def poll_sensor(channel):
    """Poll MCP3002 ADC
    Args:
        channel (int): ADC channel 0 or 1
    Returns:
        int: 10 bit value relating voltage 0 to 1023
    """
    assert 0 <= channel <= 1, 'ADC channel must be 0 or 1.'

    # First bit of cbyte is single=1 or diff=0.
    # Second bit is channel 0 or 1
    if channel:
```

```

        cbyte = 0b11000000
    else:
        cbyte = 0b10000000

    # Send (Start bit=1, cbyte=sgl/diff & odd/sign & MSBF = 0)
    r = spi.xfer2([1, cbyte, 0])

    # 10 bit value from returned bytes (bits 13-22):
    # XXXXXXXXX, XXXX####, #####XX
    return ((r[1] & 31) << 6) + (r[2] >> 2)

def sensor():
    channel = 0
    channeldata = poll_sensor(channel)
    now = time.strftime("%H:%M:%S")
    sensor = W1ThermSensor()
    temp = sensor.get_temperature()

    volt = float((channeldata * 5000) / 1024)
    if volt <= 4:
        volt = 0
    else:
        pass

    irr = float((volt*1200)/5000)

    f.write(str(now)+",")
    f.write(str(temp)+","+str(volt)+","+str(irr)+",")
    #print("Temp (Cel): {}".format(temp))
    #print("Voltage (mV): {}".format(volt))

```

```
#print('Irradiance : {}'.format(irr))

g = geocoder.ip('me')
location = g.latlng

while True:
    now = datetime.now()
    year = str(now.year)
    month = str(now.month)
    day = str(now.day)
    hour = str(now.hour)

    exists_year = os.path.isdir('/home/pi/log/'+year)
    if exists_year:
        pass
    else:
        os.chdir('/home/pi/log/')
        os.mkdir(year)

    exists_month = os.path.isdir('/home/pi/log/'+year+'/'+month)
    if exists_month:
        pass
    else:
        os.chdir('/home/pi/log/'+year+'/')
        os.mkdir(month)

    file = (day+"-"+month+"-"+year)
```

```
exists = os.path.isfile('/home/pi/log/'+year+'/'+month+'/'+ file +'_S'+'.csv')
if exists:
    pass
else:
    f = open ('/home/pi/log/'+year+'/'+ month +'/' + file +'_S'+'.csv','a+')
    f
    f.write("location"+", "+str(location))
    f.write(", "+"\\n")
    f.write("Time"+", "+ "Temp"+", "+ "Voltage(mV)"+" , "+ "Irradiance
(W/m2)"+" , ")
    f.close

now = time.strftime("%H:%M:%S")
sec = int(time.strftime("%S"))

if (sec%10 == 0):
    f= open ('/home/pi/log/'+year+'/'+month+'/'+ file +'_S'+'.csv','a+')
    f.write(", "+"\\n")
    sensor()
    f.close()
    time.sleep(5)
```